

CHAPTER II

THEORY

2.1 Molecular Sieves

With the recent discoveries of molecular sieve materials³³ containing other elements in addition to, or in lieu of, silicon and aluminum, the casual interchange of the terms “molecular sieve” and “zeolite” must be reconsidered. In 1932 McBain proposed the term “molecular sieve” to describe a class of materials that exhibited selective adsorption properties. He proposed that for a material to be a molecular sieve, it must separate components of a mixture on the basis of molecular size and shape differences. Two classes of molecular sieves were known when McBain put forth his definition: the zeolites and certain microporous charcoals. The list now concludes the silicates, the metasilicates, the metalloaluminates, the aluminophosphates (AlPO_4), metalloaluminophosphates (MeAPO), the silicoaluminophosphates (SAPO) and metallosilicoaluminophosphates (MeSAPO), as well as the zeolites. The different classes of molecular sieve materials are listed in Figure 2.1. All are molecular sieves, as their regular framework structures will separate components of a mixture on the basis of size and shape differences. The difference lies not within the structure of these materials, as many are structurally analogous, but in their elemental composition. Therefore, all are molecular sieves though none but the aluminosilicates should carry the classical name zeolites.

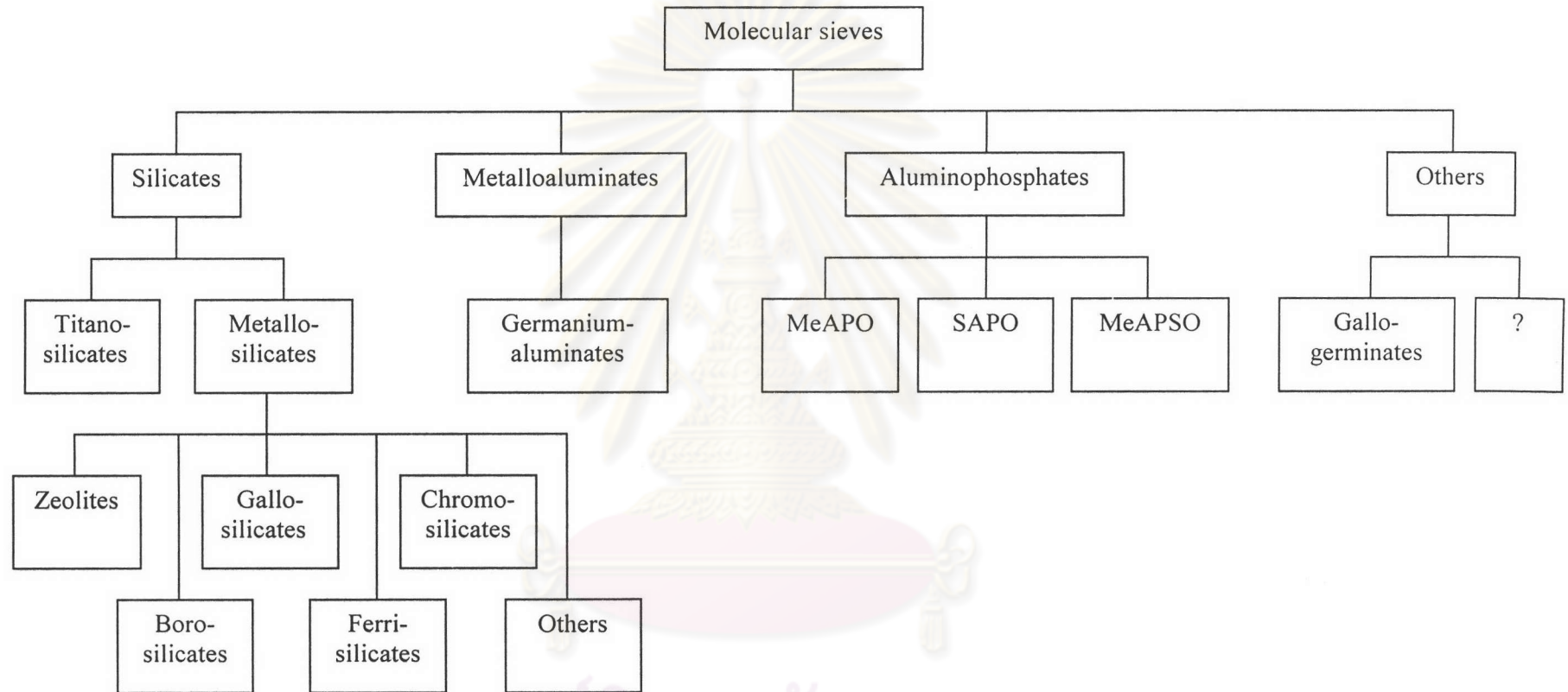


Figure 2.1 Classification of molecular sieve materials including the extensive variation in composition. The zeolites and ferrisilicates occupy a subcategory of the metallosilicates.³³

2.2 Zeolites

Zeolites^{33,34} are crystalline, hydrated aluminosilicates of group I and group II elements, in particular, sodium, potassium, magnesium, calcium, strontium and barium. Structurally the zeolites are “framework” aluminosilicates, which are based on an infinitely extending three-dimensional network of AlO_4 and SiO_4 tetrahedra linked to each other by sharing all of the oxygens as shown in Figure 2.2.

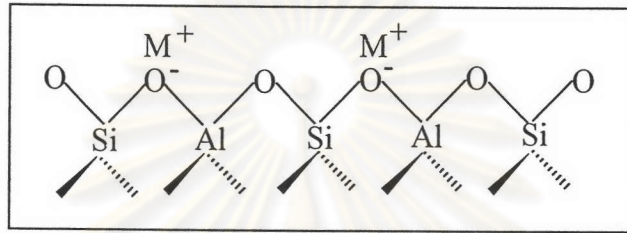
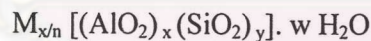


Figure 2.2 The structure of zeolites.³³

The AlO_2^- tetrahedra in the structure determine the framework charge. This is balanced by cations that occupy nonframework positions. The general formula for the composition of zeolites is



Where M is the cation of valence n, generally from the group I or II ions, although other metals, nonmetals, and organic cations are also possible, w is the number of water molecules. Water molecules presented are located in the channels and cavities, as are the cations that neutralize the negative charge created by the presence of the AlO_2^- tetrahedral unit in the structure.

2.3 Structures of Zeolites

Zeolites³³⁻³⁵ have a common subunit of structure so called primary building units of $(\text{Al,Si})\text{O}_4$ tetrahedra as revealed in Figure 2.3.

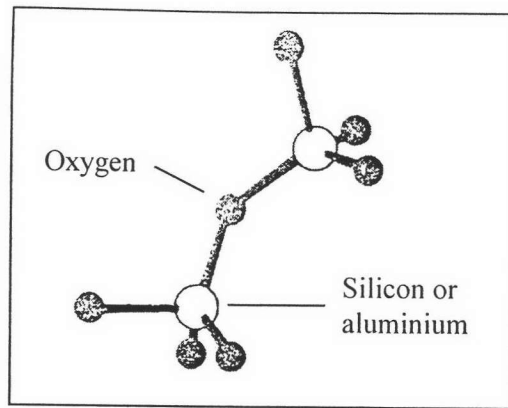


Figure 2.3 The primary building units of zeolites. Two $\text{SiO}_4/\text{AlO}_4$ tetrahedra are linked by corner-sharing.³⁵

Many zeolite structures are based on a secondary building unit (SBU) which consists of selected geometric groupings of these tetrahedra. There are nine such building units, which can be used to describe all of the known zeolite structures. The secondary building units consist of 4, 6 and 8-member single ring, 4-4, 6-6 and 8-8 member double rings, and 4-1, 5-1 and 4-4-1 branched rings as illustrated in Figure 2.4.

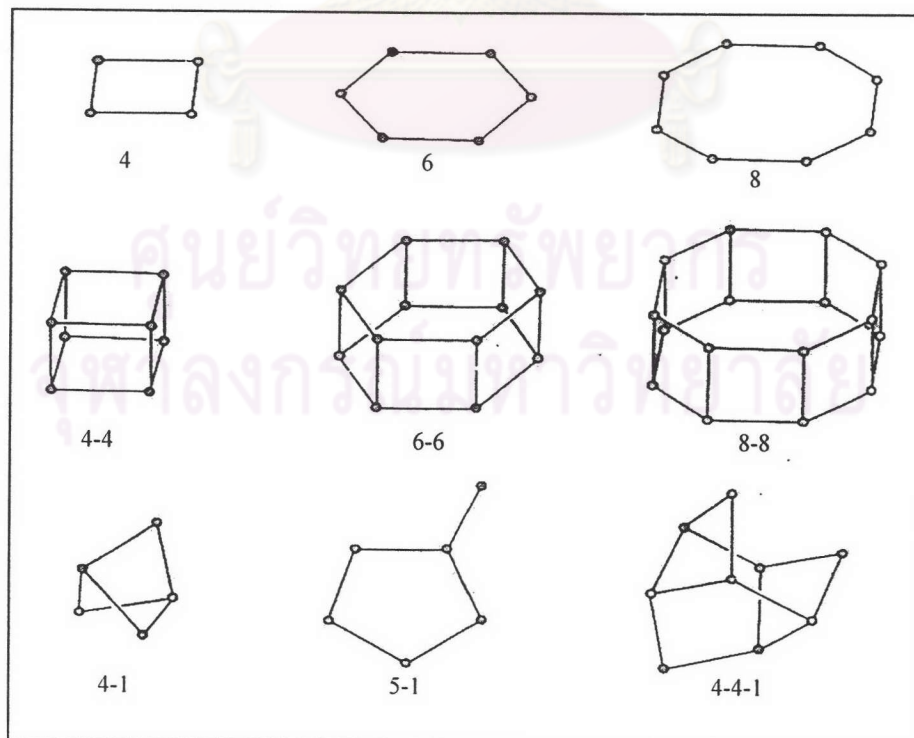


Figure 2.4 Secondary building units found in zeolite structures.³³

In some cases, the zeolite framework can be considered in terms of polyhedral units, such as the truncated octahedron (sodalite cage or β cage) as shown in Figure 2.5. Several of the most important zeolite structures are based on the sodalite unit, for example zeolite A. The sodalite units are stacked in primitive packed array and they are linked by oxygen bridges between the 4-rings. A three-dimensional network of linked cavities forming channels is thus formed which are an 8-ring window. Moreover, faujasite-type zeolite is formed by the sodalite units, which are linked by oxygen bridges between four of the eight 6-rings in a tetrahedral array, forming hexagonal prisms. The tetrahedral array encloses a large supercage (also known as an α -cage) which is entered through a 12-ring window.

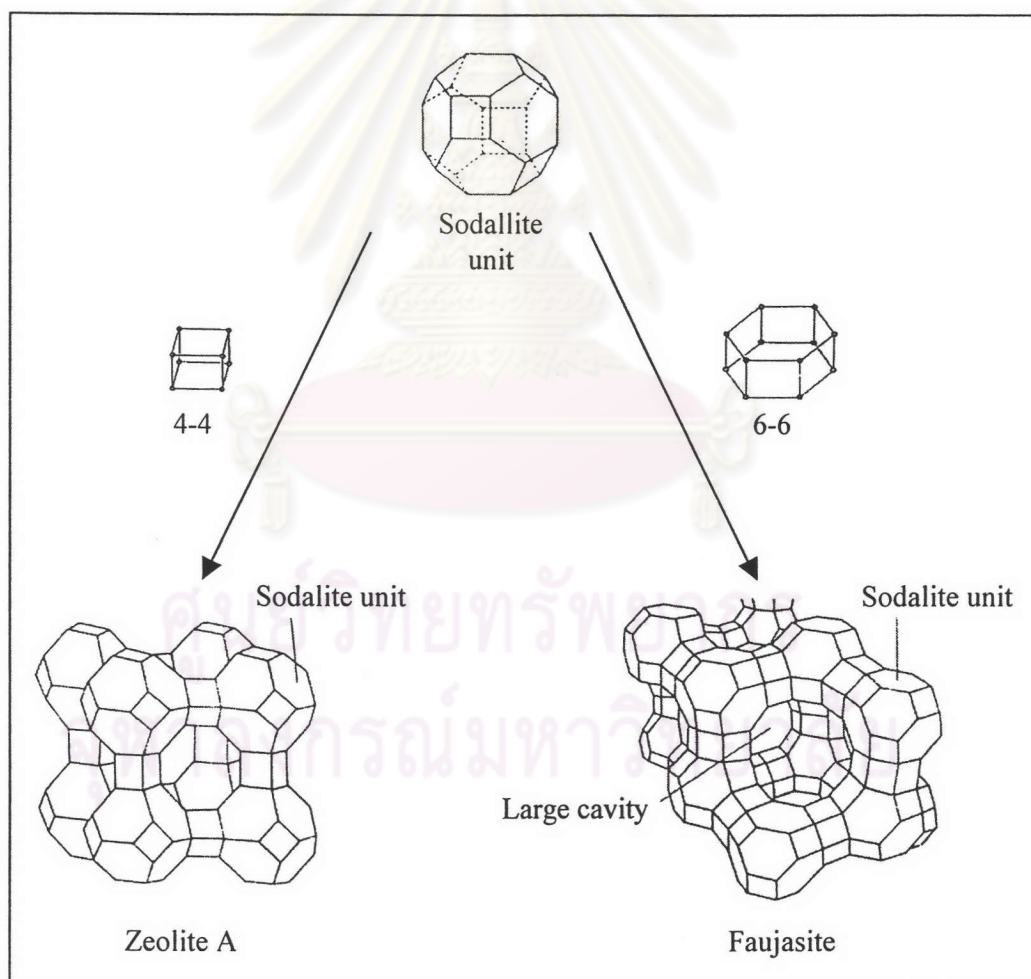


Figure 2.5 The sodalite unit and the structures of zeolite A and faujasite-type zeolites.³⁵

The secondary building unit does provides a convenient method for topologically describing and relating different zeolites. The use of the extended chain composed of the secondary building unit also simplifies visualization of certain aspects of the zeolite structure. An example of such structural mixing within a zeolite framework is the intergrowth of zeolite ZSM-5 and ZSM-11. The chain-building unit of both ZSM-5 and ZSM-11 is shown in Figure 2.6. The difference between these two zeolite structures is the way the chain-building units link to generate the structure. ZSM-5 is generating such that the chains forming sheets are related through a center of inversion, while ZSM-11 is generated through linkage such that the sheets are related through a mirror plane (not shown).

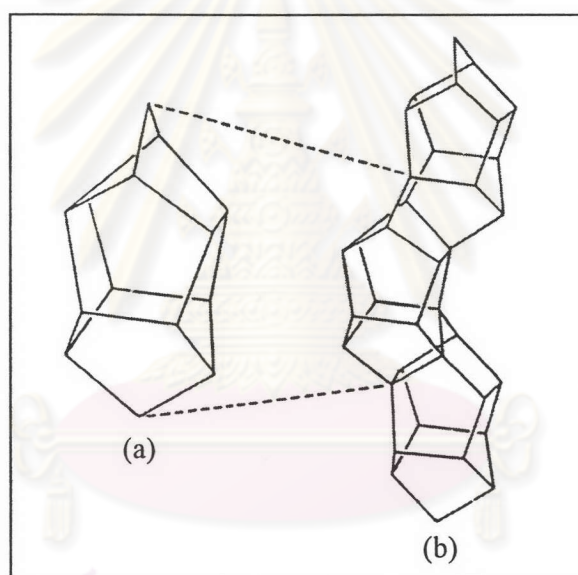


Figure 2.6 The 5-1 secondary building unit (a) to form the chain units (b) found in the ZSM-5 and ZSM-11 structures.³³

2.4 Acid Sites of Zeolites

Most industrial application of zeolites are based upon technology adapted from the acid silica/alumina catalysts originally developed for the cracking reaction.³⁵ This means that the activity required is based upon the production of Brønsted acid sites arising from the creating ‘hydroxyls’ within the zeolites pore structure. These hydroxyls are formed by ammonium exchange followed by a calcination step. Zeolites as normally synthesized usually have Na^+

balancing the framework charges, but these can be readily exchanged for protons by direct reaction with an acid, giving hydroxyl groups, the Brønsted acid sites. Alternatively, if the zeolite is not stable in acid solution, it is common to use the ammonium, NH_4^+ , salt, and then heat it so that ammonia is driven off, leaving a proton. Further heating removes water from Brønsted site, exposing a tricoordinated Al ion, which has electron-pair acceptor properties; this is identified as a Lewis acid site. A scheme for the formation of these sites is shown in Figure 2.7. The surfaces of zeolites can thus display either Brønsted or Lewis acid sites, or both, depending on how the zeolite is prepared. Brønsted sites are converted into Lewis sites as the temperature is increased above 500°C , and water is driven off.

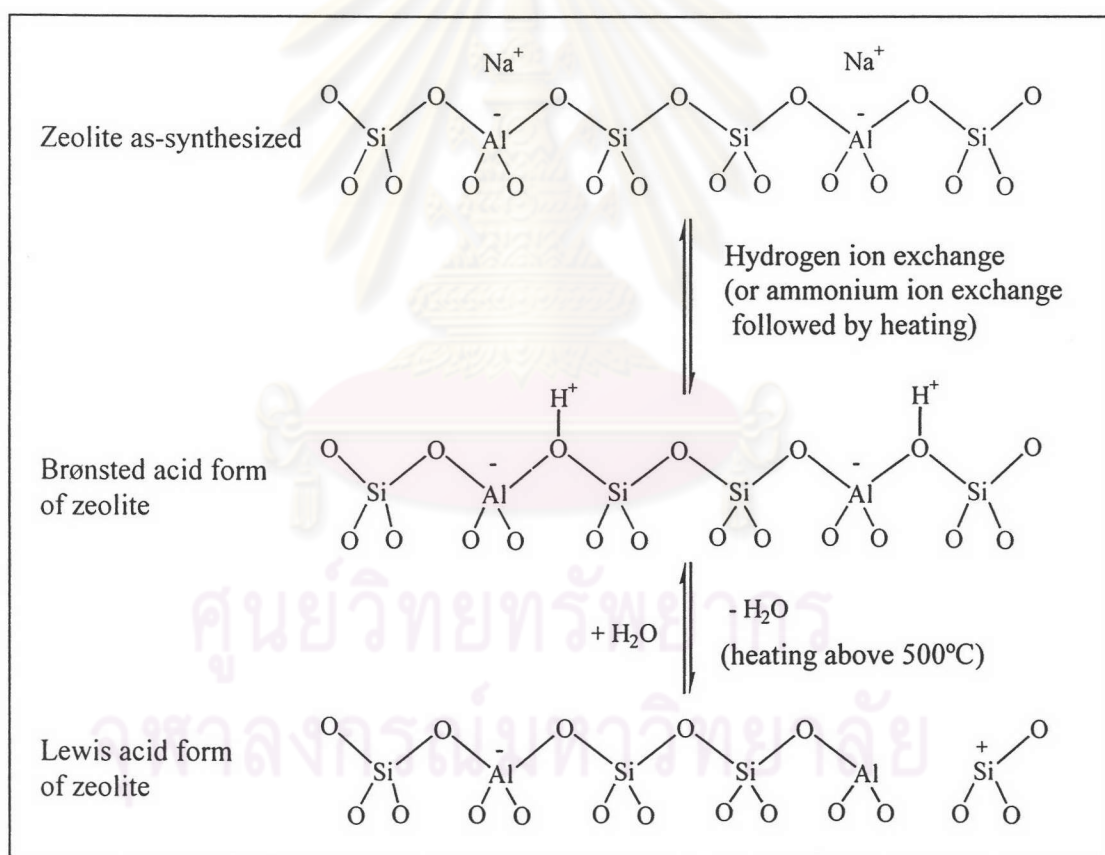


Figure 2.7 The generation of Brønsted and Lewis acid sites in zeolite.³⁶

2.5 Shape Selectivity of Zeolites

Shape selectivity³³ plays a very important role in zeolite catalysis. Highly crystalline and regular channel structures are among the principal features that zeolites used as catalysts offer over other materials. Shape selectivity is divided into 3 types: reactant shape selectivity, product shape selectivity, and transition-state shape selectivity. These types of selectivities are depicted in Figure 2.8.

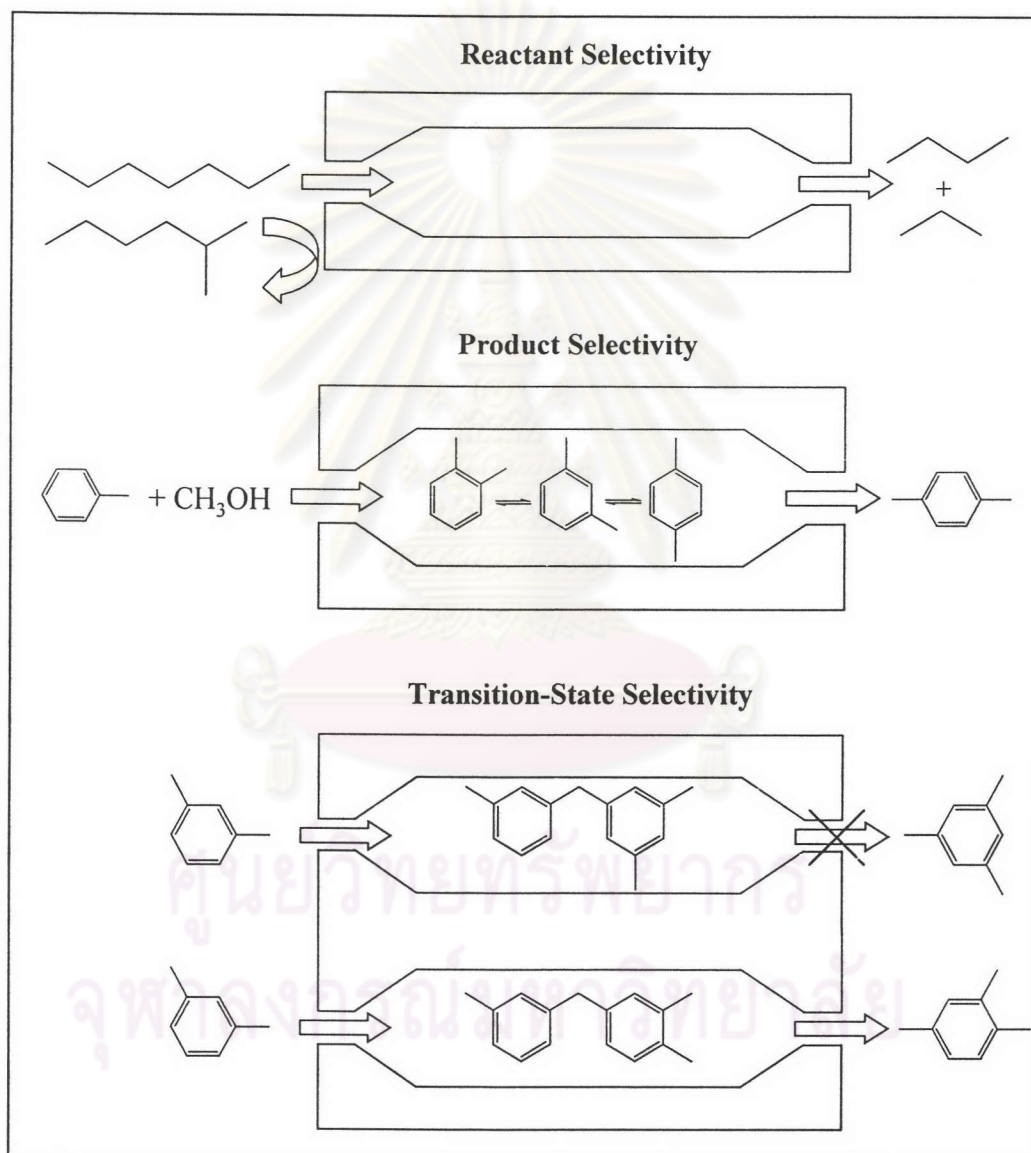


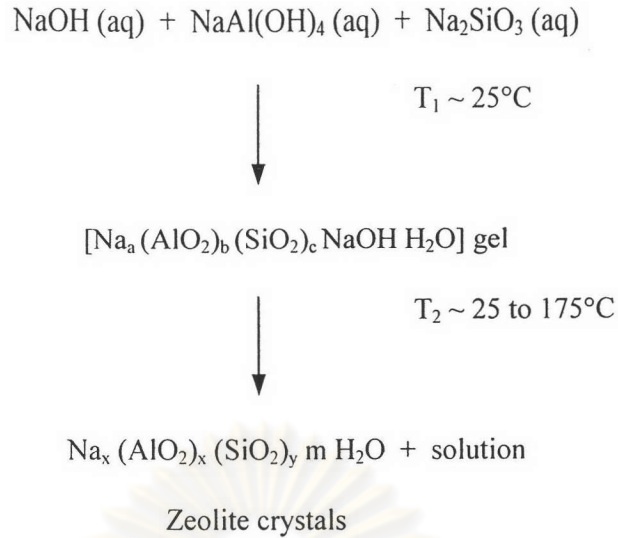
Figure 2.8 Three types of selectivity in zeolites: reactant, product and transition-state shape selectivity.³³

Reactant selectivity³⁶ is observed when only a fraction of the reactant has access to the active sites because of molecular sieving effects, while product selectivity occurs when only some product species with proper dimensions (or shape) can diffuse out of the zeolite intracrystalline volume. Restricted transition-state selectivity will take place when certain reactions will be prevented as the transition-state necessary for them to proceed will not be reached due to steric and space restrictions.

Diffusion will of course play a role of paramount importance. Those molecules with high diffusivity will react preferentially and selectively, while molecules which are excluded from the zeolite will only react on the external non-selective surface of zeolite only, due to their diffusivity is zero. Products with high diffusivity will be preferentially desorbed while the bulkier molecules will be converted and equilibrated to smaller molecules, which will diffuse out, or eventually to larger (partially dehydrogenated) species, which will block the pores. The later will lead to a progressive deactivation of the catalysts by carbonaceous residues laydown (*i.e.* coke).

2.6 Zeolite Synthesis

Zeolites are generally synthesized by the hydrothermal method in a closed cylindrical vessel, so called an autoclave. Mixing sources of aluminum, sodium, and silicon in water results in gel of four-component system $\text{Na}_2\text{O}-\text{Al}_2\text{O}_3-\text{SiO}_2-\text{H}_2\text{O}$.^{33,35} The gel is crystallized in an autogeneous pressure autoclave at temperatures varying, generally, from room temperature to about 200°C. The pressure is generally the autogeneous pressure approximately equivalent to the saturated vapor pressure of water at the temperature crystallized. The time required for crystallization varies from a few hours to several days. The alkali metals from the source of sodium form soluble hydroxides, aluminates, and silicates. These species are well suited for the preparation of homogeneous mixture. The aluminosilicate gel is formed by a process of copolymerization of the silicate and aluminate species that takes place *via* a condensation mechanism. The gel composition and zeolites structure appear to be controlled by size and structure of the polymerizing species.



A schematic representation of the crystallization of an amorphous aluminosilicate gel to a zeolite³⁴ is depicted in Figure 2.9. The gel structure, represented in two dimensions, is depolymerized by the hydroxyl ions, which produce soluble aluminosilicate species that may regroup to form the nuclei of the ordered zeolite structure. In this case the hydrated cation acts as a template.

2.7 Factors Influencing Zeolite Formation

Three variables have a major influence on the zeolite structure crystallized: the gross composition of the reaction mixture, temperature, and time.³³ There are also history-dependent factors such as digestion or aging period, stirring, nature (either physical or chemical) of the reaction mixture, and order of mixing.

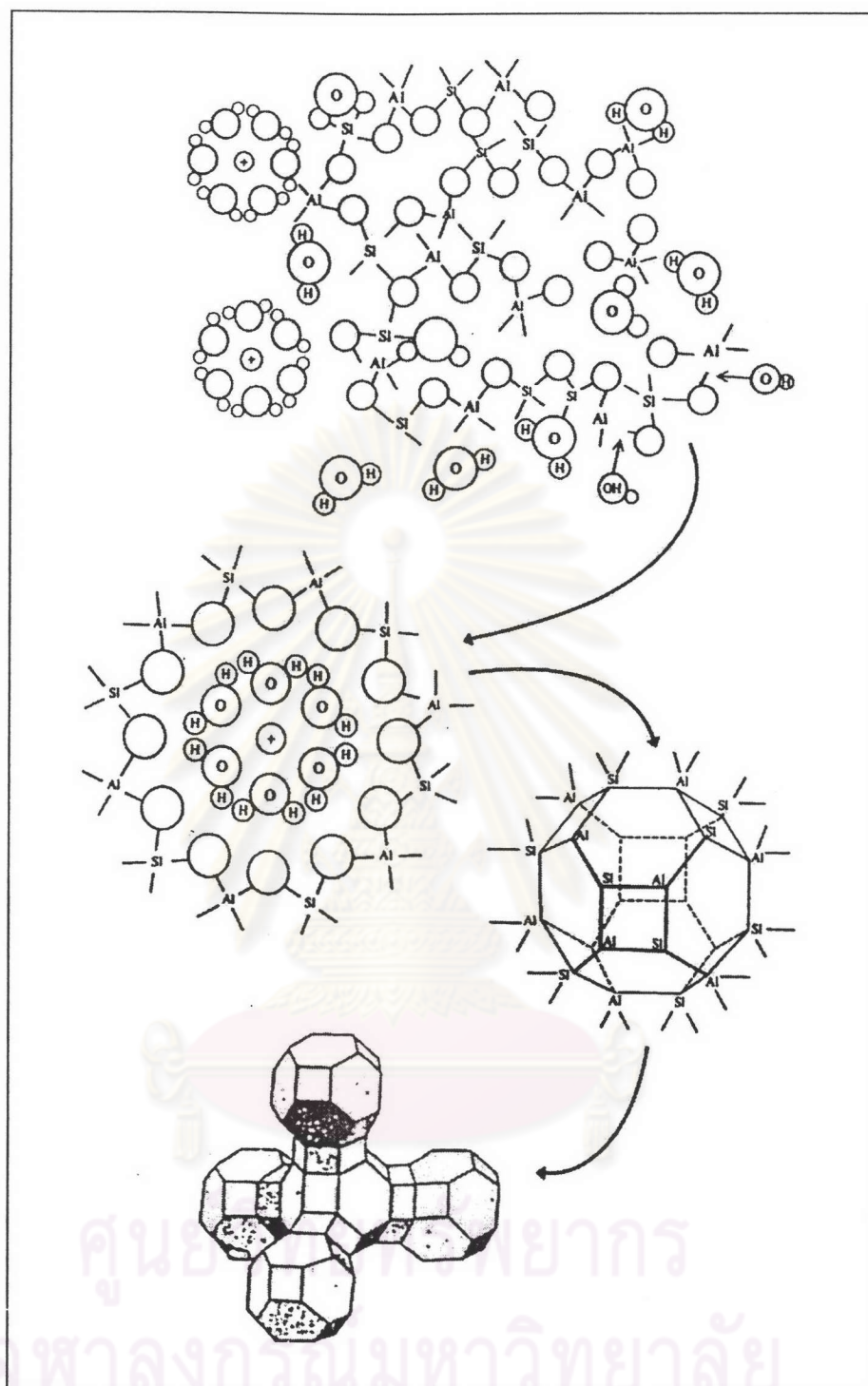


Figure 2.9 Schematic representation of the formation of zeolite crystal nuclei in a hydrous gel.³⁴

Table 2.1 Factors influencing zeolite crystallization³³

-
- Gross composition
 1. $\text{SiO}_2/\text{Al}_2\text{O}_3$
 2. $[\text{OH}^-]$
 3. Cations
 - (a) Inorganic
 - (b) Organic
 4. Anions (other than $[\text{OH}^-]$)
 5. $[\text{H}_2\text{O}]$
 - Time
 - Temperature
 1. Ambient - ca. 25 to 60°C (natural zeolite formation)
 2. Low - ca. 90 to 120°C
 3. Moderate - ca. 120 to 200°C
 4. High - ca 250°C or higher
 - History-dependent factors
 1. Aging
 2. Stirring
 3. Nature of mixture
 4. Order of mixing
-

2.7.1 Reaction Mixture Components

Each component in the reactant mixture contributes to specific characteristic of the gel and to the final material obtained. Table 2.2 provides a broad listing of individual components of the mixture and the primary influence each component has within that reactant mixture.

Table 2.2 The effects of selected variables of gross composition on the final crystalline product in zeolite synthesis³³

Variables	Primary influence
$\text{SiO}_2/\text{Al}_2\text{O}_3$	Framework composition
$\text{H}_2\text{O}/\text{SiO}_2$	Rate, crystallization mechanism
OH^-/SiO_2	Silicate molecular weight, OH^- concentration
Inorganic cation(s)/ SiO_2	Structure, cation distribution
Organic additives/ SiO_2	Structure, framework aluminum content

The $\text{SiO}_2/\text{Al}_2\text{O}_3$ mole ratio, the hydroxide content of the gel, and the presence of inorganic cations, also contribute to determining which structure(s) would finally crystallize besides the organic additives as crystal-directing agent or template.³³ For example, zeolite ZSM-5 generally crystallized in the TPA^+ (tetrapropylammonium cation) system at the ratio $\text{SiO}_2/\text{Al}_2\text{O}_3$ between 20 and infinity. However, at ratio below 20 the mordenite phase appears, will do so with or without the presence of the organic quaternary amine. Even though the tetrapropylammonium cation was considered to be a strong structure director, the presence of quantities of aluminum in the crystallizing gel, depending on the conditions used. The crystallization of a particular zeolite structure from the gel system containing these four components strongly depends on the $\text{SiO}_2/\text{Al}_2\text{O}_3$ ratio of the starting gel mixture. The inorganic or organic cations influence not only the structure crystallized but also other features of the final crystalline products produced, such as morphology and crystal size.

2.7.2 Temperature

Temperature³³ influences several factors in zeolite synthesis; it can alter the zeolite phase obtained as well as change the induction period before the start of crystallization. This induction period decreases with increasing temperature. Conditions may favor formation of other phases when the temperature is changed. For any mixture as the temperature increases, the rate of crystallization increases. The solubilities of aluminate and

silicate species also increase, causing a shift in the concentration of the liquid phase. Loosen zeolites prefer crystallization at lower temperature while denser zeolites do at higher temperature.

2.7.3 Time

Time,³³ as a parameter, can be optimized in the synthesis of many zeolites. In systems, which produce only one zeolite phase, optimizing maximum crystallization over a short span of time is important. Crystallization parameters must be adjusted to minimize the production of the other phase while also minimizing the time needed to obtain the desired crystalline phase.

2.8 Zeolite ZSM-5

The oil company Mobil first synthesized ZSM-5, Zeolite Socony Mobil-five, in 1972 and its structure code is MFI.^{33,35-38} The tetrahedral are linked to form the chain-type building block as shown in Figure 2.6. Ring consisted of five oxygen atoms are evident in this structure; the name pentasil is therefore used to describe it. ZSM-5 is a medium-pore zeolite having an orthorhombic crystalline structure. The pore opening is composed of a 10-member ring. The ZSM-5 framework contains two types of intersection channels: one type is straight, has elliptical (0.51-0.58 nm) openings, and run parallel to the b-axis of the orthorhombic unit cell, while the other has near-circular (0.54-0.56 nm) openings, is sinusoidal (zigzag) and directed along the a-axis. Figure 2.10 exhibits structure of ZSM-5 and schematic of three-dimensional channel.

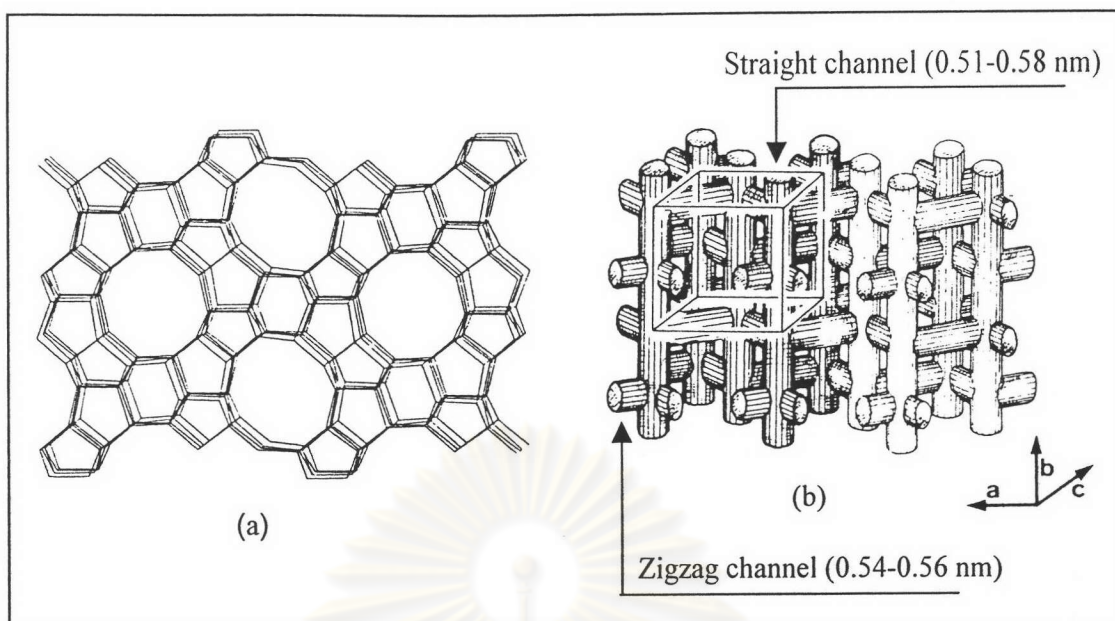


Figure 2.10 (a) Structure of ZSM-5 (MFI). View shows the straight channel. The sinusoidal channels run perpendicular to the straight channels.³⁸

(b) Schematic illustration of the three-dimensional channels in ZSM-5.³⁶

2.8.1 Shape Selectivity Properties of Zeolite ZSM-5

The accessibility to the catalytic sites in ZSM-5 is best viewed by considering its channel system as schematized in Figure 2.10(b).³⁶ The particular shape-selective properties of ZSM-5 result from the conjugation of four different structurally interrelated features:

(a) A channel (or pore) opening consisting of 10-member oxygen rings which is intermediate between that of classical shape-selective zeolites (such as Erionite, Ferrierite, Gmelinite, Chabazite, or zeolite A) and that of large pore zeolites (such as Faujasite, Mordenite, and Fault-free Offretite) as shown in Figure 2.11. ZSM-5 accepts, by decreasing order of preference, normal paraffins, isoparaffins, other monomethyl-substituted paraffins, monocyclic aromatic hydrocarbons (eventually substituted by no more than three methyl groups), and to a much smaller extent dimethyl-substituted paraffins.

The methanol to gasoline (MTG) conversion process is a good example of transition-state shape selectivity, where the available space in the cavities of zeolite ZSM-5

determines the largest bimolecular reaction complexes that can form. Hence, all products have fewer than 11 carbon atoms, with xylenes predominating.

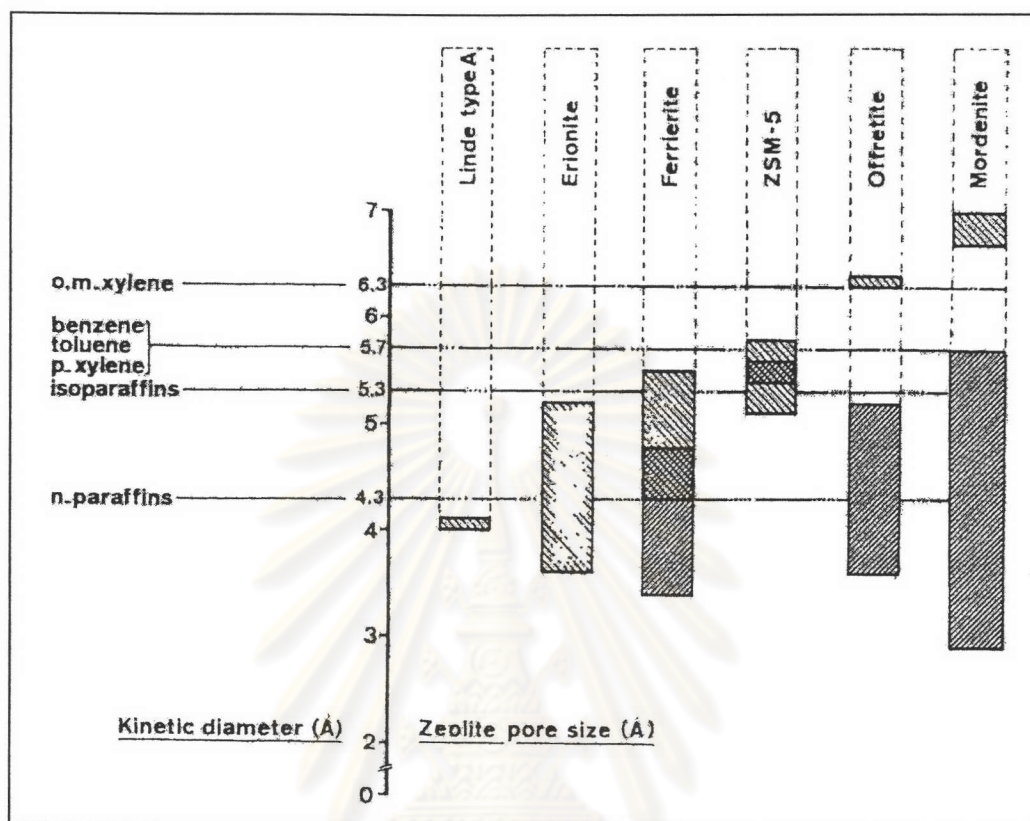


Figure 2.11 Correlation between pore size of various zeolites and kinetic diameter of some molecules.³⁶

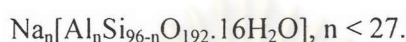
(b) The presence of channel intersections (or intersecting elements) which offer a free space of larger dimensions (about 0.9 nm); the letter may play a distinct role in the ordering of simple molecules and could be the locus for catalytic activity. Namely, Valyon *et al.*³⁶ have shown that two $n\text{-C}_3$ to C_5 aliphatic molecules can be adsorbed simultaneously at each intersecting element compared to only one for the isoparaffins and $n\text{-hexane}$.

(c) The absence of cages along the channels; such cages which offer a larger available space may be detrimental to catalytic activity, as shown in the case of Erionite, being the preferential locus for the formation of carbonaceous residues.

(d) The occurrence of slightly differentiated channel networks. Aromatics and branched paraffins were indeed found to preferentially adsorb in the linear channels which are elliptical. This may lead to preferential diffusion paths and eventually prevent major counter diffusion effects.

2.8.2 Chemical Composition of Zeolite ZSM-5

The chemical formula of a typical unit cell of hydrated Na-ZSM-5 is



There seems to be a limit on the Al incorporation in the framework. The lowest Si/Al ratio known in the ZSM-5 lattice is 10.

Zeolite ZSM-5 was used in many industrially catalytic processes and had been the subject of extensive research.³⁸ Since the catalytic activity of the material was inextricably linked to its composition and structure, recent work attempted to modify these properties by introducing heteroatoms, such as Fe, B, Ti, Ga, and Ge into the framework. For example, Fe-ZSM-5 has been prepared with varying compositions, having typical $\text{SiO}_2/\text{Fe}_2\text{O}_3$ ratios of the order of 20 to 200. Indeed, it is shown that all the iron is incorporated in the framework sites in materials with a $\text{SiO}_2/\text{Fe}_2\text{O}_3$ ratios greater than 50 and that the average iron content is 0.7 Fe per unit cell.

2.9 Fe-MFI Catalyst

Fe-MFI is a ferrisilicate of which Fe is isomorphously substituted for Si in the MFI lattice.³⁹ This results in changing in the chemical and physical properties, and inducing new catalytic activities. Figure 2.12 reveals Si and Fe in the MFI structure. Like Al, Fe atoms in the zeolitic framework cause the appearance of negative charge in the framework, which must be compensated by cations or protons in the form of bridged hydroxyls (Brønsted acid site).

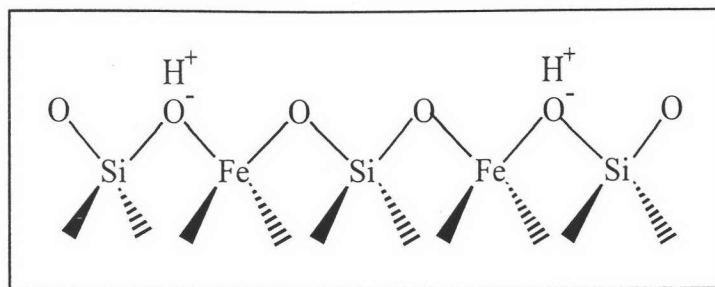


Figure 2.12 The structure of Fe-MFI.³⁹

Iron cations can be incorporated into the tetrahedral framework sites of a MFI structure during the ferrisilicate synthesis. Although the degree of iron substitution is generally very low, it is dependent on the synthetic condition.^{40,41} Irons not only necessarily occupy exclusively the framework sites of ferrisilicate but also exist in the ion exchange sites as charge balancing cation and also in the ferrisilicate cavities as the small iron oxide particles. Some of techniques such as Mössbauer,⁴²⁻⁴⁶ ESR,^{39,47-68} IR,^{59,69} UV^{50,59} and EXAFS⁷⁰ are commonly used to characterize these iron sites.

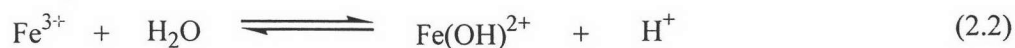
2.9.1 Factors for Synthesis of Ferrisilicates

There are two methods for synthesis of iron-containing molecular sieves. The difference between two methods is the addition step of iron source. The first one is direct synthesis. Silica source, iron source and template were mixed prior to crystallization. The other one is post synthesis. Silicalite-1, which is the pure-silica form of ZSM-5 zeolite, was prepared. Then, iron source was added and crystallization was performed at the same temperature. Nevertheless, direct synthesis is more useful compared to post synthesis because the former has more iron in the framework position than the latter.⁷¹ Thus, direct synthesis was used to synthesize ferrisilicate molecular sieves in this work.

During synthesis of ferrisilicate molecular sieves the objective is to incorporate Fe³⁺ ions into the growing lattice framework made up of silica tetrahedral. To achieve this, the reaction leading to the formation of ferrisilicate complex as shown in equation (2.1)⁷² should be favored:



The ferrisilicate complex has to be enhanced, while that leading to the formation of hydroxides of iron, equation (2.2), has to be suppressed.



This can be accomplished by complexing the iron with silica at low pH using an aluminum-free source of Si and choosing the raw material and reaction condition to maximize the concentrations of monomeric/short chain silicate species. As seen early, above pH of 4, insoluble iron hydroxide species are formed. Therefore, it is not easy to incorporate these polymeric species of iron in a growing silicate network. Hence, the monomeric/short chain silicate species is usually added to an acidic solution (pH below 4) containing the Fe^{3+} ions in order to form the ferrisilicate complexes. Once all the irons are complexed with the silicates to form the ferrisilicates, the pH of the reaction mixture can be safely increased to values needed for the synthesis of zeolitic structure without the precipitation of the rust-red iron hydroxides. The organic base is added after the formation of the ferrisilicate gel. After adjusting pH to the desired value, the amorphous gel was converted into the crystalline structure in an autoclave at elevated temperature.

In addition, three factors^{40,41,72,73} appear to be critical in consistent and proved successful in preparation of ferrisilicate molecular sieves over a wide range of Si/Fe ratios as shown in the following sections.

2.9.1.1 The Avoidance of Iron Hydroxide Precipitation

Iron tends to precipitate as rust-red colloidal ferric hydroxide at pH value above 4.^{40,41} Once formed, ferric hydroxide is almost completely insoluble, hence limiting the availability of FeO_2^- species for being incorporated into silica units during crystal growth. This problem is not encountered in zeolite synthesis, since any colloidal aluminum hydroxide formed redissolves more readily at the pH necessary for zeolite crystallization. The ability of Fe^{3+} to precipitate silica species through complex formation was reported in early studies of silicate and soil chemistry. Complex was formed between the two species at pH

values of 3 and 4. Therefore, initial formation of a ferrisilicate complex at low pH avoids precipitation of rust-red iron hydroxide. Once the iron is complexed in this manner, the formation of ferric hydroxide at elevated pH appears to be suppressed. The pH is then adjusted with OH^- (as NaOH) to the conditions necessary to promote molecular sieve crystallization. Upon addition of the silica-containing solution to the acidic Fe^{3+} solution, distinct color changes are observed with changing pH. Below pH 3, the solution is bright yellow, turning turbid and peach color around pH 4. The solution rapidly increases in opacity with this appearance of color when above pH 6. The final pH used in this synthesis is between 8-11. Within this range the opaque gels are either white or pale yellow, depending on the amount of iron used in the formation of the gel. The yellow gel disappears upon crystallization, resulting in highly crystalline white materials.

However, the content of the framework iron is mostly dependent on the final pH of the final synthesis gel. Kyu-Wan *et al.*⁷³ studied the pH effect (pH of 8 to 11) on the preparation of MFI type ferrisilicate zeolites. They found that the optimum pH for synthesis of the highly incorporated iron ferrisilicates is around 8, while for pH of the synthesis gel at 7 or below, the crystallinity was lost after calcination for 5 h at 500°C.

2.9.1.2 The Necessity of Using Low Molecular Weight Silica Source

The amount of silica needed to react with all the iron depended on the extent of polymerization within that silica source. Sodium metasilicate and N-brand silicate,^{40,41} both consisting of a low-molecular-weight silica species produce good-quality white to pale yellow gels with $\text{SiO}_2/\text{Fe}_2\text{O}_3$ as low as 5 to 8 in the preparation of Fe-MFI. On the other hand, Ludox and Cab-O-sil,^{40,72} containing 200 Å particles of high-molecular-weight polymeric silica beads, are not found to be effective. A rust-red gel indicative of the presence of hydroxide of iron was obtained in these cases. When this gel was crystallized, under conditions suitable for the synthesis of the ZSM-5 structure, a brown solid was obtained, which contained significant quantities of occluded iron oxide. The lattice framework consisted essentially of silicate wherein only a limited amount of iron was incorporated in

tetrahedral, framework sites. The majority of the iron was in octahedral (non-framework) sites. Prolonged digestion of the silica particles in NaOH, which breaks the silica polymers into smaller units, increased iron incorporation. Tetraethyl orthosilicate (TEOS) is another preferred source of Si. A major advantage in the use of TEOS as the source of Si is that impurities can be excluded. Other sources of Si (like sodium silicate, silica gel, silica sol *etc.*) invariably contain trace quantities of Al and lead to ferrialumino-silicate compositions during synthesis.

2.9.1.3 The Need to Suppress the Formation of Iron Complexes With Organic Amine

The presence of a complexing template or crystal-directing agent, which binds strongly the Fe^{3+} species, also prevents it from forming the ferrisilicate gel.⁴¹ For example, a strongly coordinating neutral amine template such as, pyridine is found to limit incorporation of the iron into the gel and the final crystalline molecular sieves structure. Non-coordinating tetrapropylammonium bromide, free of the neutral amine impurity, does not appear to impede incorporation and is the template of choice in crystallizing the ZSM-5 structure.

2.9.2 Thermal Stability of Ferrisilicates

For silicalite-1, a pure silica analogue of the ZSM-5 series, crystal stability to 1300°C in dry air is observed.⁴¹ The ferrisilicate analogue also exhibits high thermal stability maintaining crystal integrity and porosity with increasing temperature. However, some iron was lost from the framework sites upon mild (500°C) thermal treatment. The ferrisilicate, as-synthesized, contains the organic TPA^+ cations trapped within a pore system. To study this material further it was necessary to remove the organic cations by thermal decomposition. The ferrisilicate was subjected to a two-step decomposition procedure, where it was first heated slowly in flowing N_2 to 550°C and maintained at that temperature for 8 h. This was followed by air calcination for 4 h, similar to the procedure for the aluminosilicate. This total

calcination procedure, reproduced in the thermal gravimetric balance, showed a major weight loss on the first step equivalent above 9 h for removal of the organic cations from the molecular sieve. Air calcination following, the residues in only a 4-5% further weight loss. Differential thermal analysis of the organic decomposition process shows that organic cations break down around 450°C. In air the reaction is strongly exothermic, resulting in indeterminate sample temperatures within the crystal. Direct air calcination, not preceded by thermal treatment under nitrogen also produces quantities of water, which may result in hydrothermal removal of some of the iron from the framework. Thermal treatment under nitrogen is mildly endothermic and provides much better control over the sample temperature as the template decomposition. Further thermal treatment in air to remove the carbonaceous residue causes minimum change in the sample temperature. By this two-step method excessive temperature variation in the sample was controlled and the possibility of hydrothermal reactions within the crystal was minimized. Moreover, Fejes *et al.*⁴⁸ supported the caring calcination. Unlike from 'standard' calcination where the as-synthesized zeolite samples were heated at about 500°C in air, 'caring' calcination means heating (3°C/min) in pure nitrogen up to 500°C in order to decompose and remove about 90-92% of organics, followed by cooling down to 400°C while maintaining the nitrogen flow. Thereafter, disconnecting the nitrogen from oven, the sample was heated up under the conditions of increasing oxygen concentration (from air) to remove the carbonaceous rest of template.

Furthermore, Pérez-Ramírez *et al.*⁷⁴ studied the effect of calcination and steam treatment (300 mbar of H₂O in N₂) on Fe, Al-ZSM-5. It was found that calcination at 550°C leads to complete removal of the template. During this process a significant fraction of iron is dislodged to extra-framework positions (ca. 50%), while Al is hardly affected. Steam treatment leads to the significant dealumination of the zeolite structure, the complete extraction of isomorphously substituted iron, and the clustering of extra-framework iron species into highly dispersed oxide nanoparticle of 1-2 nanometers, containing Fe and probably Al. Steam treatment of Fe, Al-ZSM-5 decreases the density and strength of acid sites and leads to mesopore formation (around 11 nanometers), whereas the apparent crystalline

structure and morphology are not altered. Figure 2.13 shows different forms of iron in Fe, Al-ZSM-5.

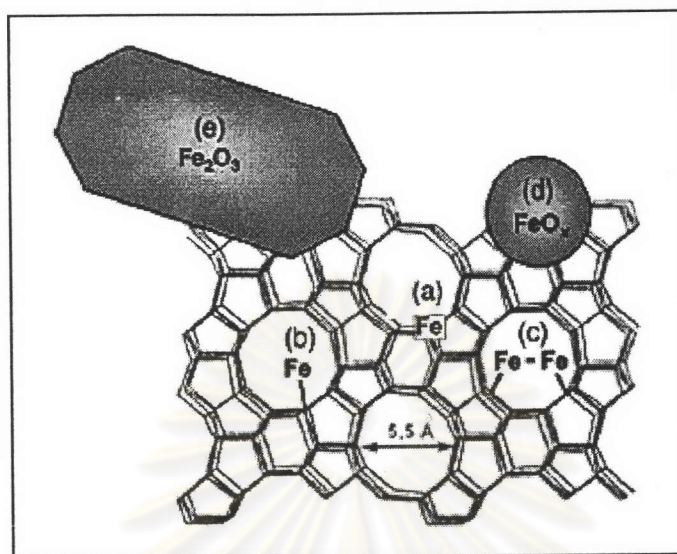


Figure 2.13 Schematic representation of the different Fe species identified in Fe-ZSM-5.⁷⁴

This includes isolated irons either:

- (a) in framework positions (isomorphously substituted),
- (b) in cationic positions in the zeolitic channels,
- (c) binuclear and in general oligonuclear iron complexes in extra-framework positions,
- (d) iron oxide FeO_x nanoparticle of size under 2 nanometers, and
- (e) large iron oxide particles (Fe_2O_3) in a wide distribution (upto 25 nanometers in size) located at the surface of the zeolite crystal.

In addition, effect of template burning at 500 and 700°C on the local Fe^{3+} environment was investigated.³⁹ The production associated water from the burning of template in Fe-silicate is sufficient to cause the partial rupture of some bonds connecting iron with the oxygens of the framework and to induce migration of the iron into extra-framework positions. Because of this, a decrease of the framework iron species and the simultaneous appearance of oxidic microaggregates were observed after calcination. For calcination at

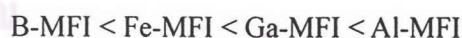
500°C, a high concentration of Fe^{3+} was still present in the zeolitic framework. On the other hand, calcination in air at 700°C caused a dramatic removal Fe^{3+} from framework towards extra-framework positions. The amount of Fe^{3+} anchored to the zeolitic framework was small and that the majority of Fe^{3+} was now in extra-framework positions, possibly in the form of oxidic microaggregates.

Therefore, the two-step calcination at 500°C was used to remove the organic template from Fe-MFI catalysts in this work due to these procedure produced high Fe^{3+} in framework positions.

2.9.3 Acidity of Ferrisilicates

The strength of acid sites in a zeolite of a given framework topology can be modified by isomorphous substitution. For silicates with the framework topology of zeolite ZSM-5 (MFI structure), isomorphous substitution can be conveniently achieved by replacing the aluminum source in the synthesis gel by other metal cations, for example Be, B, In, Cr, Ga, Cr, V, Sc, Ge, Mn, La, Ni, Zr, Ti, Fe, Co, and Pt.^{29,69,75-77} This results in a great modification of the acidic properties of the molecular sieves.

Figure 2.14 shows NH_3 -TPD profiles of various metallosilicates having MFI structure.⁶⁹ The acid strength of metallosilicates, indicating by the temperature of desorped NH_3 of maximum rate, increases as follows:



Moreover, FTIR results show that the band positions of OH changes in conformity with NH_3 -TPD result.⁶⁹ Based on the observed OH frequencies, the Brønsted acidity of the bridging hydroxyls was therefore ordered as follows:



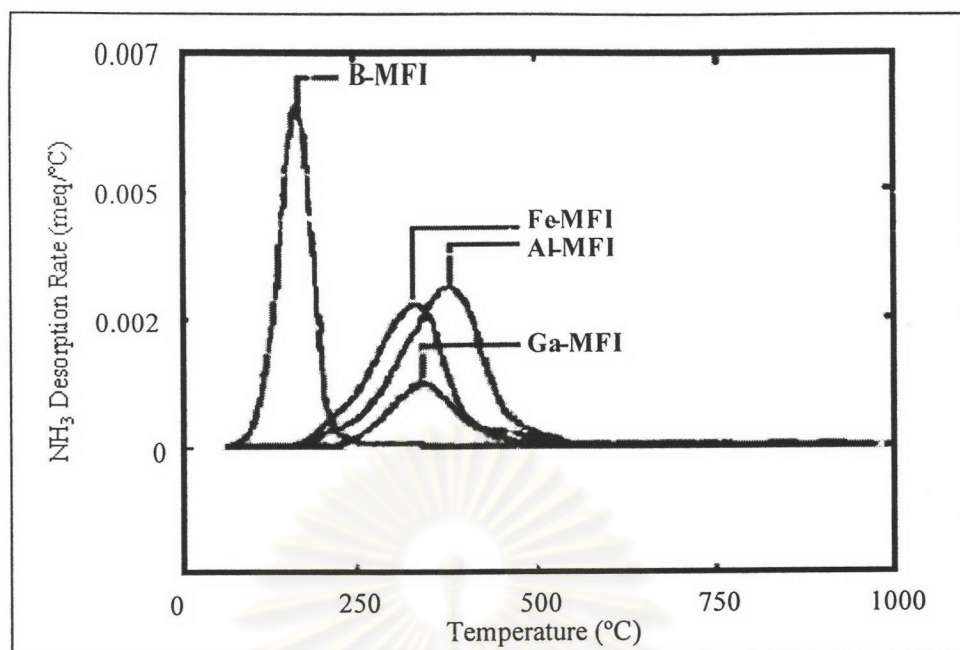


Figure 2.14 NH_3 -TPD profiles of isomorphous ZSM-5.⁶⁹

A variety of metallosilicates containing different kinds of transition metals were synthesized by adopting the rapid crystallization method, and performance of those metallosilicates for methanol conversion was compared with that of protonated Al-silicate, *i.e.*, H-ZSM-5.²⁶ NH_3 -TPD profiles for those typical metallosilicates showed that the high temperature peaks correspond to the strong acid sites and were responsible for the hydrocarbon conversion. The order of the strength was as follows:

$$\text{Al-silicate} > \text{Ga-silicate} > \text{Fe-silicate}$$

As a result, significant difference in the catalytic performance of these catalysts was found. H-Ga-silicate showed has a high activity for very selective aromatization. The acid strength of H-Ga-silicate was rather weaker than on H-ZSM-5 as mention above, aromatization progressed more and still the formation of light paraffinic hydrocarbons were much less than those on H-ZSM-5. On the other hand, H-Fe-silicate exhibited its performance that selective formation of ethylene and propylene from methanol. Thus, Fe-silicate was an attractive MTO catalyst.

2.9.4 Characterization of Iron in Ferrisilicates by ESR Spectroscopy

Since Fe^{3+} ions is paramagnetic in both the low-spin and high-spin electronic configurations,⁵⁰ ESR spectroscopy should be a good method for characterizing the iron sites in zeolites where the weak ligand field of the possible ligands (water, hydroxide, framework oxygen) results in high-spin ferric states. In this case, the interpretation of the ESR spectra is difficult due to complications associated with inhomogeneous broadening arising from the zero field splitting (ZFS) and overlapping signals. The X-band ESR spectrum of zeolites containing Fe^{3+} usually consists of three major signals at $g \approx 4.3$, $g \approx 2.2$ - 2.3 , and $g \approx 2.0$. The commonly accepted assignment of these signals has been as follows: framework iron, iron in interstitial oxide or hydroxide phases, and iron in cation-exchange sites, respectively.^{39,45-68} The appearance of a signal at $g \approx 4.3$ has often been used as evidence for framework substitution in zeolites and AlPO_4 .^{53,56,59}

The spin Hamiltonian of low-spin Fe^{3+} , $S = 1/2$, is dominated by the electronic Zeeman interaction with a highly anisotropic g factor. The ESR spectrum thus consists of a single transition, and in orientationally disordered samples it shows a characteristic powder. In contrast the spin Hamiltonian of high-spin Fe^{3+} , (d^5 , $S = 5/2$) include the ZSF interaction as well as the electron Zeeman interaction, which is shown in equation (2.3):^{50,55}

$$H = g\beta B_0 S + D[S_z^2 - 1/3(S(S + 1))] + E(S_x^2 + S_y^2) \quad (2.3)$$

Where β is the Bohr magneton, B_0 is the external magnetic fields vector, S is the spin vector of Fe^{3+} ions, and D and E are the axial and rhombic distortion parameters of the ZSF interaction. The ZFS parameters D and E , measure the deviations of the ion crystal field from the ideal tetrahedral or octahedral symmetry, *i.e.* “cubic” fields, for which both $D = 0$ and $E = 0$.^{50,68} When $D = 0$ and $E = 0$, an isotropic signal of $g \approx 2.0$ or slightly greater value is observed. If the symmetry of the field is lower, say axial, with $D \neq 0$ and large and $E = 0$, an anisotropic signal is observed with $2.0 < g \leq 6.0$. If the symmetry is reduced further to fully rhombic with $D = 0$ and $E \neq 0$, this results in a seemingly “isotropic” signal at $g \approx 4.3$. This

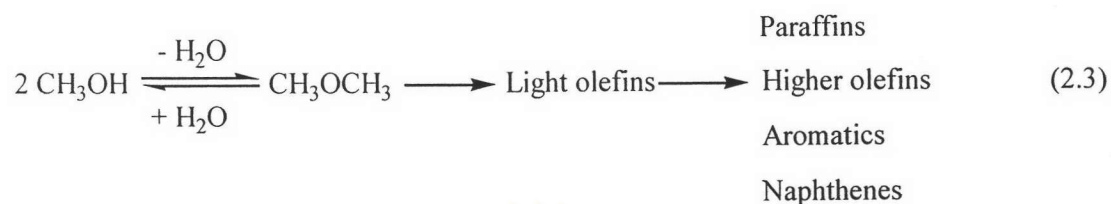
signal corresponds to Fe^{3+} in tetrahedral coordination MA_2B_2 (C_{2v}), distorted octahedral MA_6 (D_{2h}) or MA_3B_3 where M = metal ion and A and B = ligands.⁵⁵

2.10 Methanol to Olefins (MTO) Process

To begin with, the methanol to hydrocarbons technology was primarily regarded as a powerful method to convert coal into high-octane gasoline.⁶ This concept has been expanded since, not only with respect to the formation of other fuels, but also to chemicals in general can be synthesized. Light olefins are important components for the petrochemical industry, and the demand for high quality gasoline is increasing as well. In fact, with this new technology, one can make almost anything out of coal or natural gas that can be made out of crude oil. Methanol is made from synthesis gas (a mixture of carbon monoxide and hydrogen), which is formed by steam reforming of natural gas or gasification of coal. It is then converted to an equilibrium mixture of methanol, dimethyl ether and water, which can be processed catalytically to either gasoline (called MTG) or olefins (called MTO), depending on the catalyst and/or the process operation condition. The commercial MTG reaction runs at the temperature around 400°C and methanol partial pressure of several bars using ZSM-5 as a catalyst. These are the optimal conditions for converting the olefins that form within the catalyst into paraffins and aromatics. However, at one point in the MTG reaction, the product mixture consists of about 40% light olefins. The importance of light olefins as intermediates in the conversion of methanol to gasoline was recognized early. Consequently, a number of attempts were made to selectively form light olefins from methanol, using zeolite as a catalysts, for example small-, medium-, large-pore zeolites, and also SAPO type molecular sieves. If one interrupted the reaction at the point of about 40% light olefin formation, one could harvest these C_2 - C_4 olefins. By adjusting the reaction conditions (such as raising the temperature to 500°C) as well as the catalyst applied, one can increase dramatically the olefins yield. This discovery led to the development of the MTO process, which generates mostly propylene and butene together, with high-octane gasoline as a byproduct. However, the catalyst can be modified in such a way that even more ethylene is produced.

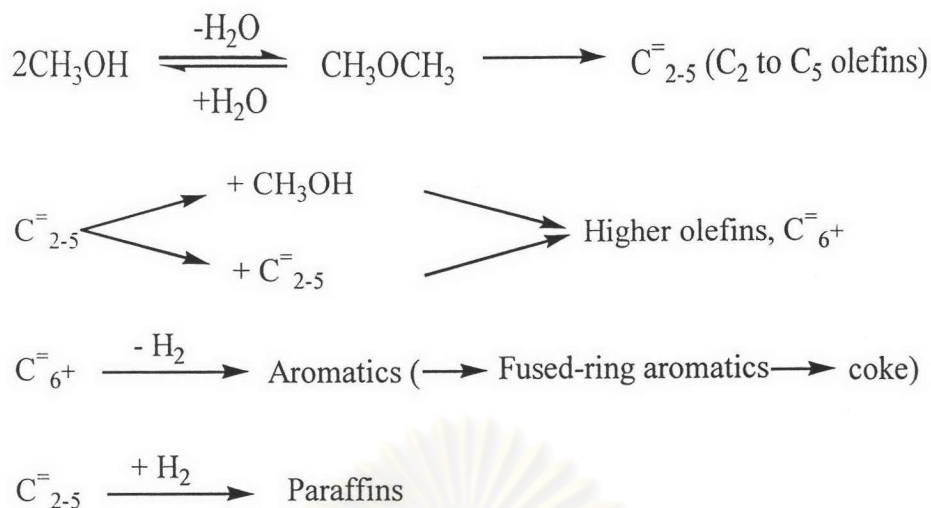
2.10.1 Reaction Mechanisms for MTO Process

The main reaction steps of the methanol conversion to hydrocarbons^{6,78,79} can be summarized as follows:



This process consists of three steps of reactions: (1) the formation of dimethyl ether (DME), (2) the initial C-C bond formation resulting in light olefins, and (3) the subsequent conversion of the primary products (light olefins) into higher olefins, and also paraffins, aromatics, and naphthenes, as shown in equation (2.3). Brønsted acidity is known to be the main source of the catalysts activity for the MTO process, while the conjugate Lewis basic site would be responsible for the initial C-C bond formation.

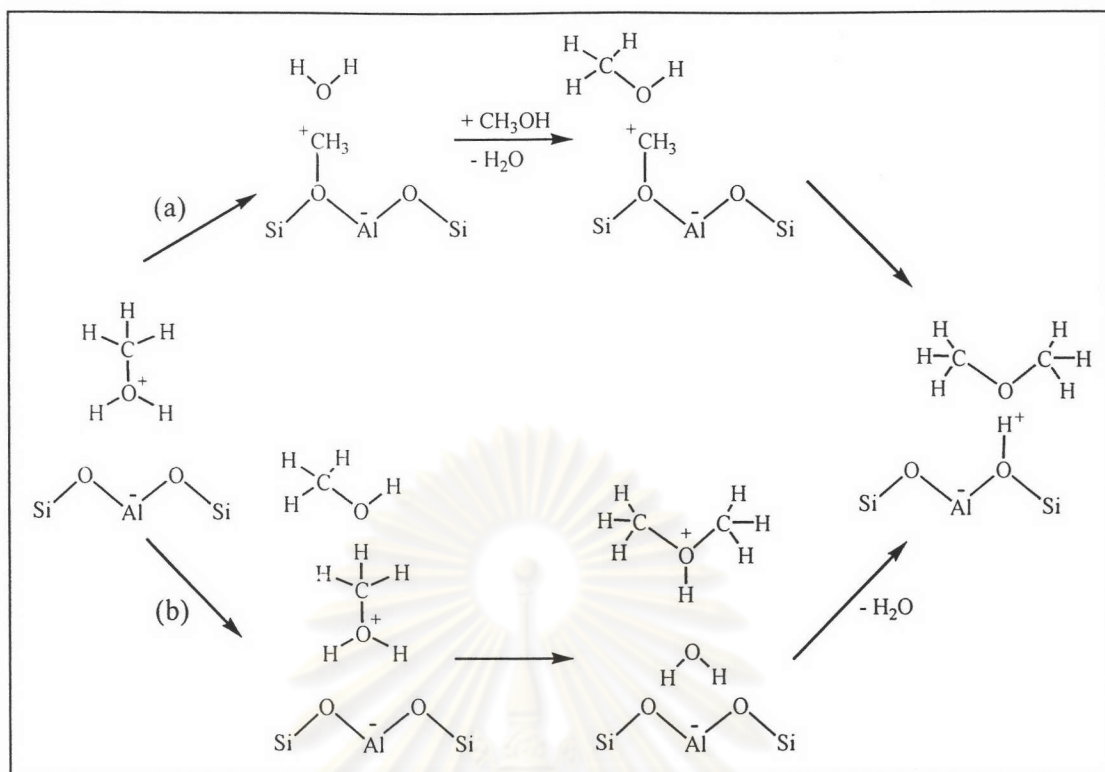
It is generally accepted, the facts that the numbers of acid sites or the amounts of strong acid sites are strictly proportional to the Al content. However, the intrinsic catalytic property as a solid acid cannot be changed by merely variation of the Al content.²⁶ Therefore, isomorphous substitution of Al with other elements producing a catalyst having different intrinsic catalytic properties is of interest. Using a pentasil type zeolite H-ZSM-5, as a catalyst in this process was the epoch finding that a high octane number gasoline can be selectively produced. This is due to the fact that H-ZSM-5 has a poor function of hydrogen release from the catalyst surface but a strong hydrogen shift function. Thus valuable intermediate compounds, light olefins, are easily hydrogenated into chemically stable and light paraffinic hydrocarbons and dehydrogenated to aromatics, as shown in Scheme 2.1.



Scheme 2.1 Reaction scheme of the methanol conversion on a typical H-ZSM-5.²⁶

2.10.1.1 Formation of Dimethyl Ether

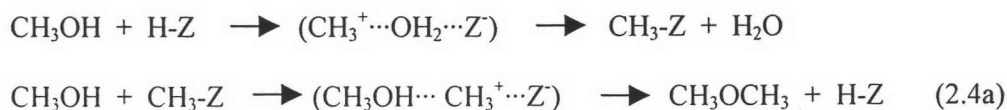
Gale *et al.*⁸⁰ suggested that the dimethyl ether formed *via* two pathways, which involving either the intermediate surface bound methoxy groups (a) or direct condensation of methanol (b), as illustrated in Scheme 2.2. In the first pathway (a), methanol undergoes nucleophilic attacked by the zeolite to form a framework methoxy species, which in turn reacted with a second molecule of methanol to form dimethyl ether. In the second pathway (b), the zeolites were not directly involved except as an acid-base “solvent”, with two methanols directly condensing. Both reaction pathways were found to be energetically reasonable based on thermodynamic criteria, which all intermediates were more stable than the isolated reactants. Although there was a spectroscopic evidence for the presence of framework bound methoxy species in zeolites under reaction conditions, it was found that the direct condensation pathway is the thermodynamically favored one.



Scheme 2.2 Two possible pathways for the formation of dimethyl ether in the presence of an aluminosilicate catalyst for MTO process.⁸⁰

According to a gas phase cluster studied of the same two pathways,⁸¹ it had also been indicated that the direct condensation (b) mechanism was preferred to path (a). The two main different pathways were as follows:

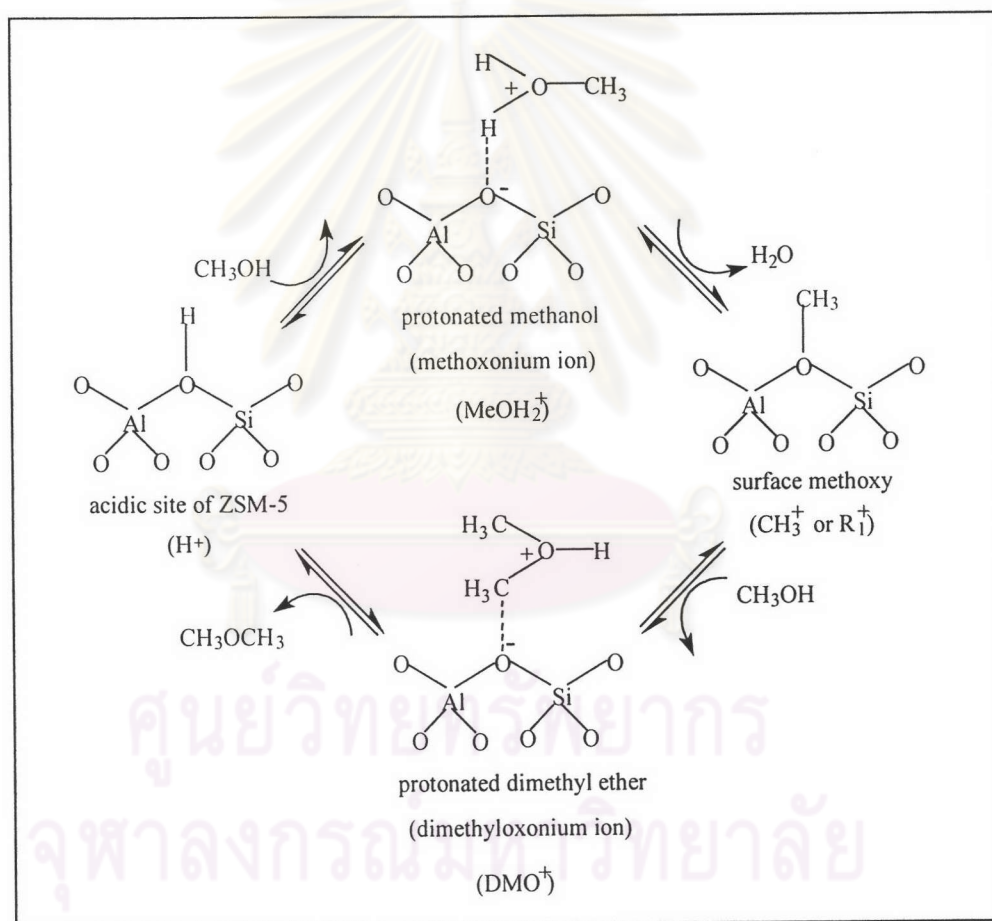
(a) Methanol was adsorbed on the active site of zeolite H-Z to form a surface methoxy, CH₃-Z, and the other methanol approached this surface-bonded methyl group to form dimethyl ether (called the Rideal-Eley mechanism), as revealed in equation (2.4a).



(b) Two methanol molecules were adsorbed simultaneously on the active site and were then dehydrated to form dimethyl ether directly, as shown in equation (2.4b).

$$2\text{CH}_3\text{OH} + \text{H-Z} \longrightarrow (\text{CH}_3\text{OH}\cdots\text{CH}_3^+\cdots\text{OH}_2\cdots\text{Z}) \longrightarrow \text{CH}_3\text{OCH}_3 + \text{H-Z} + \text{H}_2\text{O} \quad (2.4b)$$

In accordance with pathway (a), the formation of dimethyl ether was investigated by the magic-angle-spinning (MAS) NMR.⁷⁹ Scheme 2.3 shows the formation of dimethyl ether. The data showed that methanol was reversibly adsorbed through hydrogen to the bridged hydroxyl on Brønsted acid sites. The protonation was very fast on strong acidic sites and was considered to reach equilibrium. The protonated methanol transformed *via* dehydration to a surface methoxy species, which was covalently bonded to the lattice oxygen of ZSM-5 and reacted in turn with other methanol to form a dimethyloxonium ion (DMO⁺). Deprotonation of the latter yielded dimethyl ether and H⁺.



Scheme 2.3 Formation of dimethyl ether during the course of MTO process.⁷⁹

2.10.1.2 Formation of initial C-C Bond

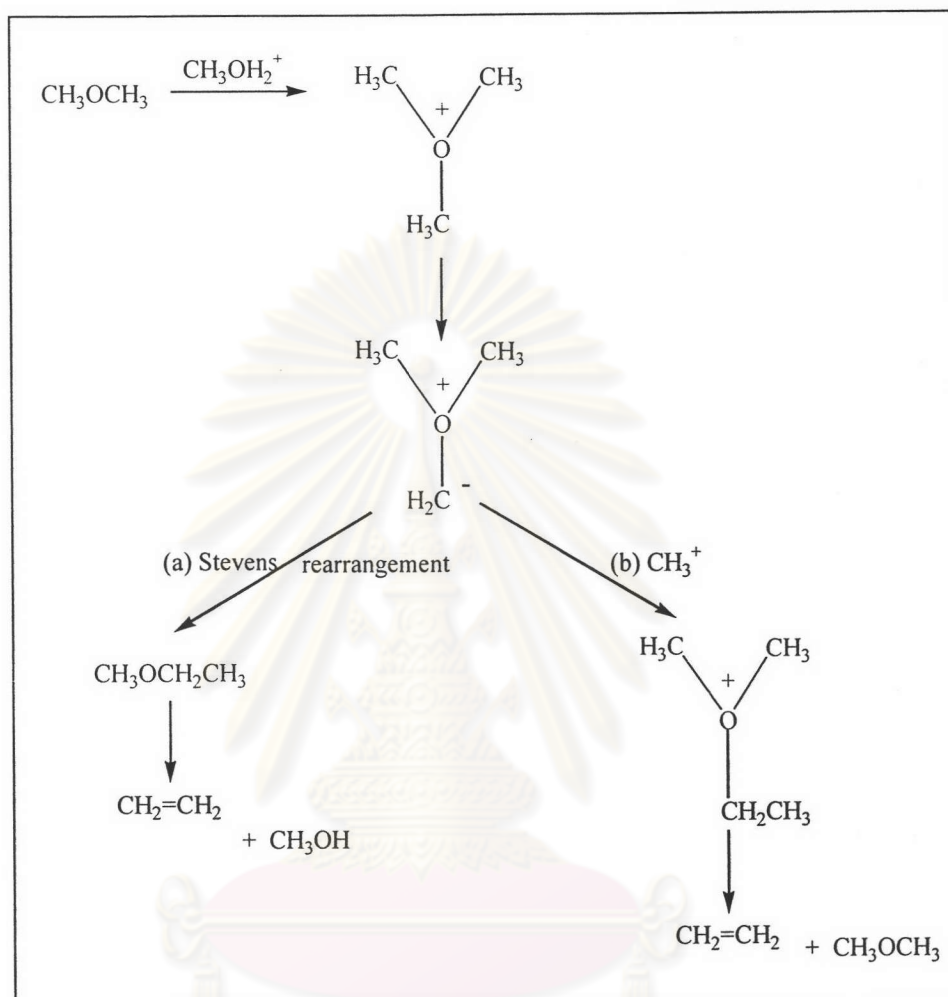
There were large number of possible reaction mechanisms for the formation of the initial C-C bond, which was regarded as a step producing primary hydrocarbon products from methanol on acid catalysts: (I) oxonium ylide, (II) carbene, (III) free radical, and (IV) hydrocarbon chain mechanism. These mechanisms established several types of C_1 intermediates: carbocationic type, which were surface methoxonium groups (CH_3^+ methyl cations) and possibly oxonium ions; carbene type ($:CH_2$), formed by the simultaneous action of acid and basic sites; and free radicals.

However, considerable discrepancies arise in the identification of the first hydrocarbon products because secondary reactions are more rapid than primary ones. Besides, they were also limited by internal diffusion in the porous structure of the catalyst. Ethylene is the sole primary product on H-ZSM-5 zeolites according to the experimental observations of Chu and Chang⁸², while Marin *et al.*¹ pointed towards ethylene and propylene as the primary gas-phase products. Different authors had also identified methane and ethylene as the only primary products on the ZSM-5 zeolites. Sulokowski and Klinowski⁸³ had identified *trans*-2-butene as a first product in the gaseous stream at low temperature.

I. Oxonium ylide mechanism

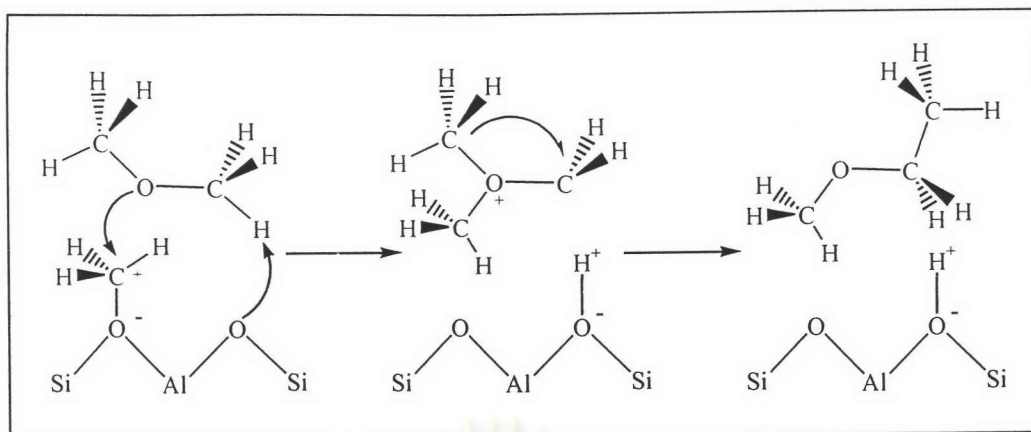
Scheme 2.4 shows the oxonium ylide mechanism in the MTO process.⁶ Dimethyl ether interacted with a protonated methanol on a Brønsted acid site on the solid catalyst to form a dimethyl oxonium ion, which reacted further with another dimethyl ether to form a trimethyl oxonium ion. This trimethyl oxonium ion was subsequently deprotonated by a basic site to form a surface associated dimethyl oxonium methyl ylide species. The next step was either an intramolecular Stevens rearrangement (a), leading to the formation of methylethyl ether, or an intermolecular methylation (b), leading to the formation of the ethyldimethyl oxonium ion. Bimolecular methylation of the dimethyl oxonium ylide resulted in the ethyldimethyl oxonium ion, rather than an intramolecular Stevens

rearrangement. In addition, a number of other investigators favor this mechanism as a result of the linear dependence of hydrocarbon formation and zeolite Brønsted acidity.

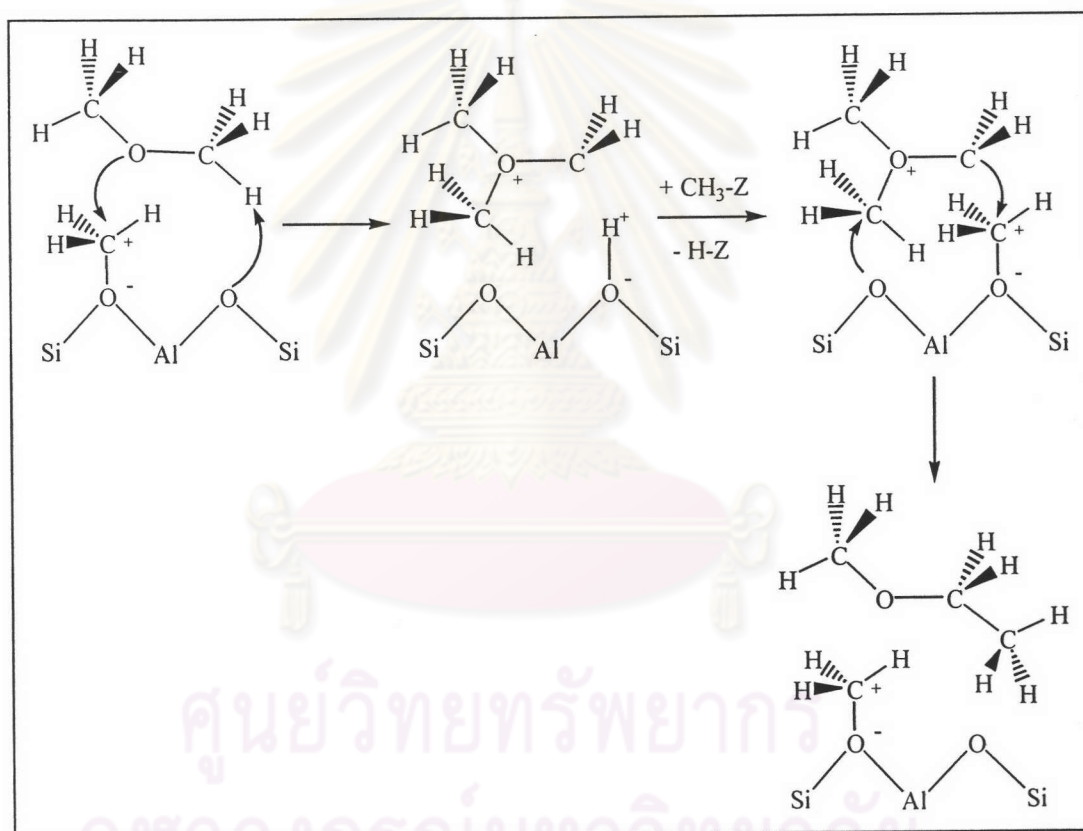


Scheme 2.4 The oxonium ylide mechanism in the MTO process.⁶

Moreover, this mechanism was suggested in the experiment by Olah *et al.*⁸¹. Scheme 2.4a and 2.4b show the oxonium ylide mechanism *via* Stevens-type rearrangement and *via* intermolecular CH_3^+ transfer, respectively. In oxonium ylide mechanism, resulted in the C-C bond formation, yielding ethyl methyl ether. Subsequently, an intramolecular rearrangement within the oxonium ylide (called the Stevens-type rearrangement mechanism) or an intermolecular transfer of the CH_3 group from surface methoxy to methylenedimethyloxonium ylide, $(\text{CH}_3)_2\text{OCH}_2$, first took place.



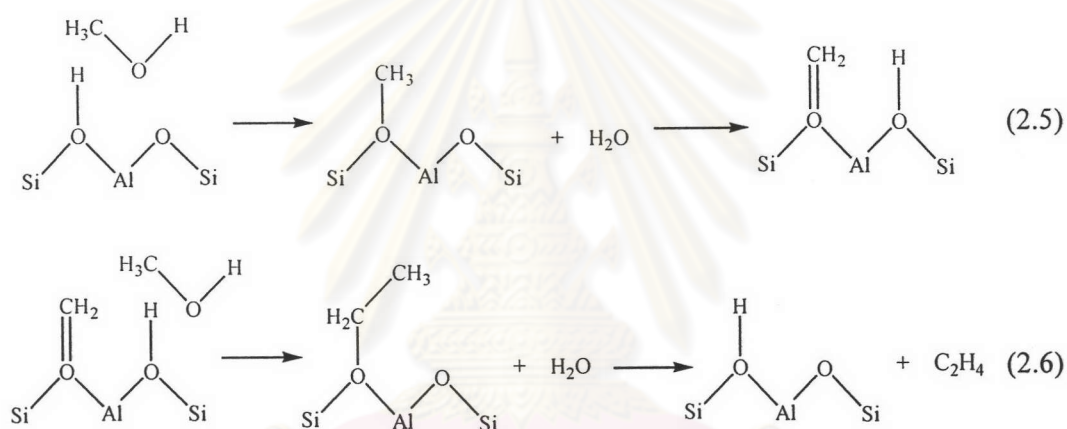
Scheme 2.4a The Stevens-type rearrangement in the oxonium ylide mechanism.⁸¹



Scheme 2.4b The intermolecular CH_3^+ transfer in oxonium ylide mechanism.⁸¹

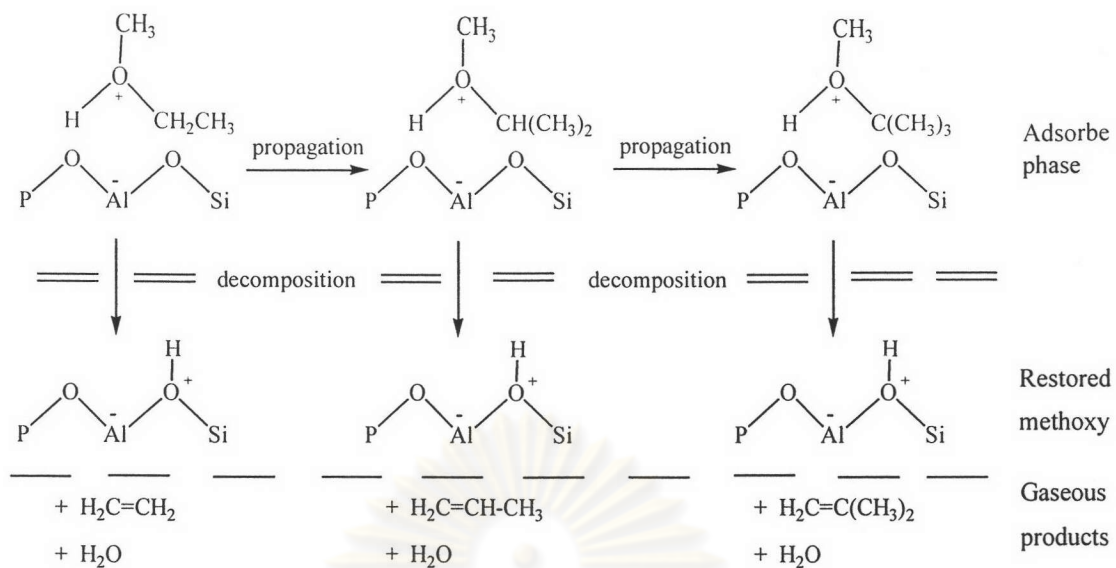
Besides the formation of dimethyl oxonium methyl ylide species as shown in Schemes 2.4a and 2.4b, a surface ylide species was proposed by Hutchings *et al.*⁸⁴ An adsorbed methanol molecule was dehydrated to form a surface-bound methoxy species a proton of which then transferred to a neighboring bridged oxygen to form a charged surface ylide nearby a Brønsted acid site. The formation of the surface methoxy in which the

surface oxygen, methyl carbon and the leaving OH group were roughly colinear follows a classic S_N2 mechanism (Eq. 2.5 in Scheme 2.5). The initial C-C bond should then be formed in a more facile reaction between a methanol (or dimethyl ether) and the surface ylide (Eq. 2.6 in Scheme 2.5), which would lead to the formation of a surface ethoxy group. Ethylene could be formed by β -elimination along with reforming the Brønsted acid site. Alternatively, the surface ethoxy species could react with further methanol molecules to form a surface isopropoxy group and subsequently a tertiary butoxy group. These surface species undergoing β -elimination would lead to the formation of propylene and *iso*-butylene, respectively.

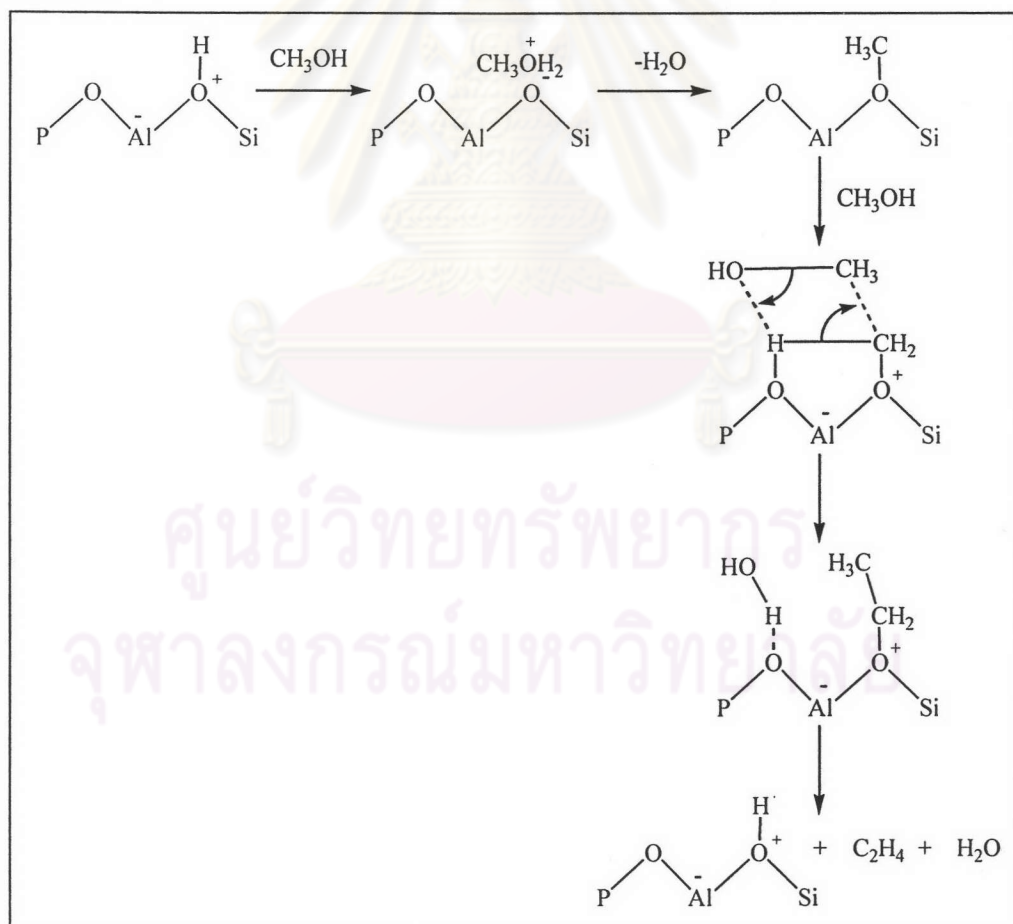


Scheme 2.5 A proposed mechanism for the formation of surface ylide species.⁸⁴

Sánchez del Campo *et al.*⁸⁵ supported the oxonium ylide mechanism for methanol transformation into olefins on SAPO-34. Form *in situ* FTIR analysis of the reaction in the catalytic chamber, it was proven that olefin formation took place *via* oxonium ion as intermediates. The oxonium ions were successively methylized by propagation reaction in solid phase resulting in the formation of ethyloxonium and propyloxonium, and so forth, which are shown in Scheme 2.6. The formation of ethyloxonium, which gave way to the formation of ethylene, is shown in Scheme 2.7.

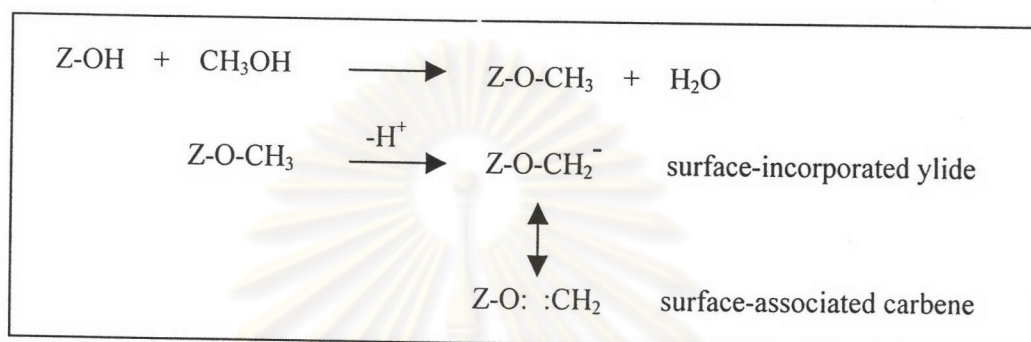


Scheme 2.6 A proposed mechanism for formation of olefins *via* methoxonium ion.⁸⁵



Scheme 2.7 Another proposed mechanism of surface oxonium ions.⁸⁵

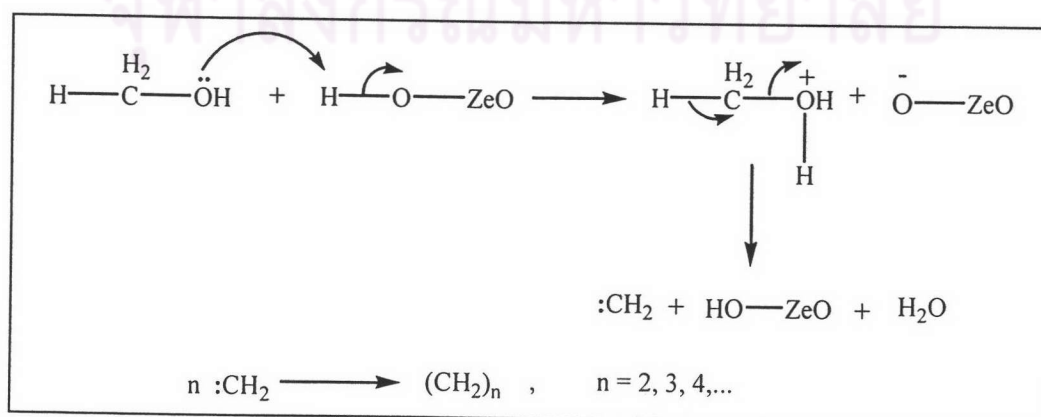
In summary, the oxonium ylide mechanism involves the formation of a surface-bound intermediate as the initial reaction step. The zeolite surface OH-group is methylated to form the methyloxonium intermediate, which gives rise to a surface-bound methylene-oxonium ylide due to deprotonation. The surface-bound methylene oxonium ylide is isoelectronic with a surface-associated carbene, as outlined in Scheme 2.8.⁶



Scheme 2.8 Summary of a proposed oxonium ylide mechanism applied to the zeolite surface.⁶

II. Carbene mechanism

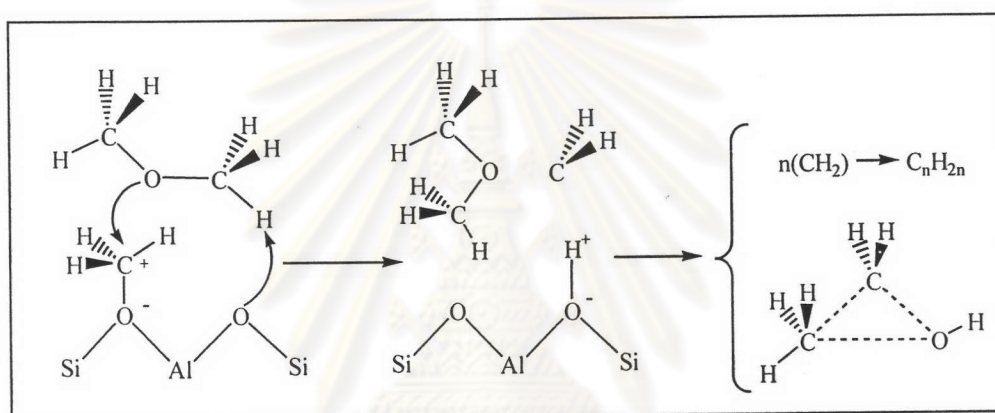
The carbene mechanism involved the α -elimination of water from methanol followed by either polymerization of the resultant carbene to olefins or by concurrent sp^3 insertion of carbene into methanol or dimethyl ether. The formation of the carbene by the cooperative action of acid and basic sites in mordenite was suggested by Swabb and Gates⁶ and can be summarized in Scheme 2.9.



Scheme 2.9 The carbene formation from methanol adsorbed on the zeolite surface.⁶

Whereas the oxonium ylide mechanism essentially involves the formation of a surface-bound intermediate as the initial reaction step, the carbene mechanism involves only surface associated intermediates. As previously mentioned the surface-associated carbene is isoelectronic with the surface-bound methylene oxonium ylide species.

Chang and Silvestri⁸¹ reported that the conversion of methanol to hydrocarbons on H-ZSM-5, favoring the carbene mechanism for the initial C-C bond formation. Scheme 2.10 shows the carbene mechanism. Methanol or dimethyl ether reacted with the surface-bonded methyl group on the active sites.

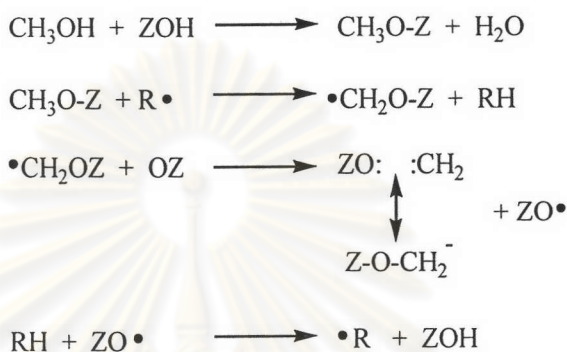


Scheme 2.10 The carbene mechanism for MTO process.⁸¹

III. Free radical mechanism

As an alternative for the formation of methyloxonium intermediates, the free radical mechanism has been also introduced. Clarke *et al.*⁶ recognized that dimethyl ether could be the source of methyl radicals whose presence was detected by ESR spectroscopy in the reaction of dimethyl ether over H-ZSM-5. Radicals are formed initially by interaction of dimethyl ether with paramagnetic centers (solid-state defects) in the zeolite and consequently the C-C bond formation results from direct coupling of radicals. The suggestion of Clarke *et al.* eliminated the requirement of strongly basic sites for proton removal from C-H, a major drawback of a number of introduced mechanisms. Evidence to support this mechanism is the observation by Change *et al.*⁶, who found that MTO was completely, but reversibly, inhibited by small amounts of NO, a well-know radical scavenger.

The author concluded that while the result confirmed the presence of free radicals, the role of these radicals in MTO initiation is an open question. Nevertheless, since dimethyl ether readily generated radicals upon gas phase pyrolysis even at MTO temperature, and since NO inhibition of dimethyl ether pyrolysis was well-known, radical-initiated MTO deserved further attention. A mechanism is shown in Scheme 2.11.



Scheme 2.11 The free radical mechanism for MTO process.⁶

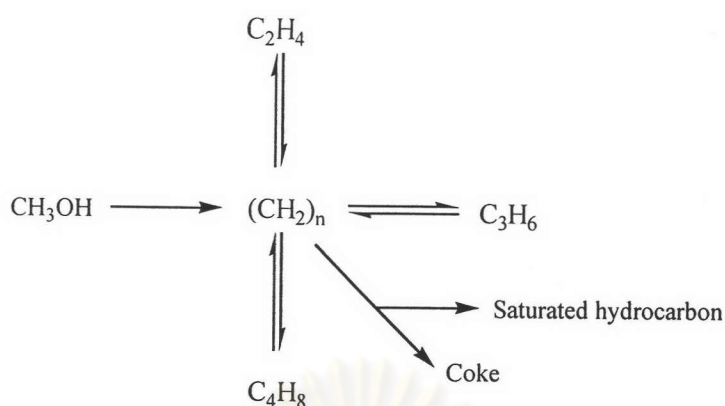
IV. Hydrocarbon Chain

The consecutive type mechanism with one carbon from methanol adding during each step,⁶ addition of methanol and cracking of olefin intermediates may take place as illustrated in Scheme 2.12.



Scheme 2.12 The consecutive-type mechanism of the hydrocarbon chain reactions.⁶

A parallel type mechanism, known as “hydrocarbon pool” mechanism was suggested by Dahl *et al.*⁸⁶⁻⁹⁰ who studied the methanol conversion to hydrocarbons using SAPO-34 as a catalyst, and ¹³C-labeled methanol and ¹²C-ethylene made *in situ* from ethanol in the reaction (Scheme 2.13).



Scheme 2.13 The parallel-type mechanism of hydrocarbon chain reaction.⁸⁶⁻⁹⁰

The “hydrocarbon-pool”, or $(\text{CH}_2)_n$, represents an adsorbate, which may have characteristic in common with ordinary coke, and which might easily contain less hydrogen than indicated. It would perhaps be better represented by $(\text{CH}_x)_n$ with $0 < x < 2$. Using SAPO-34 in the methanol conversion reaction, the product pattern is simpler than the case of using ZSM-5, where a much wider range of products was found. Therefore, it might be easier to obtain a picture of the reaction pathway using SAPO-34, and the authors showed that the consecutive mechanism, as far as propylene formation was concerned, did not turn out to be valid. Only a minor part of the propylene molecules might have been formed by addition of methanol to ethylene since this would imply a $^{12}\text{C}/^{13}\text{C}$ ratio larger than one. In fact, the ratio seemed to be lower, thus the majority of the propylene molecules should be formed directly from methanol.

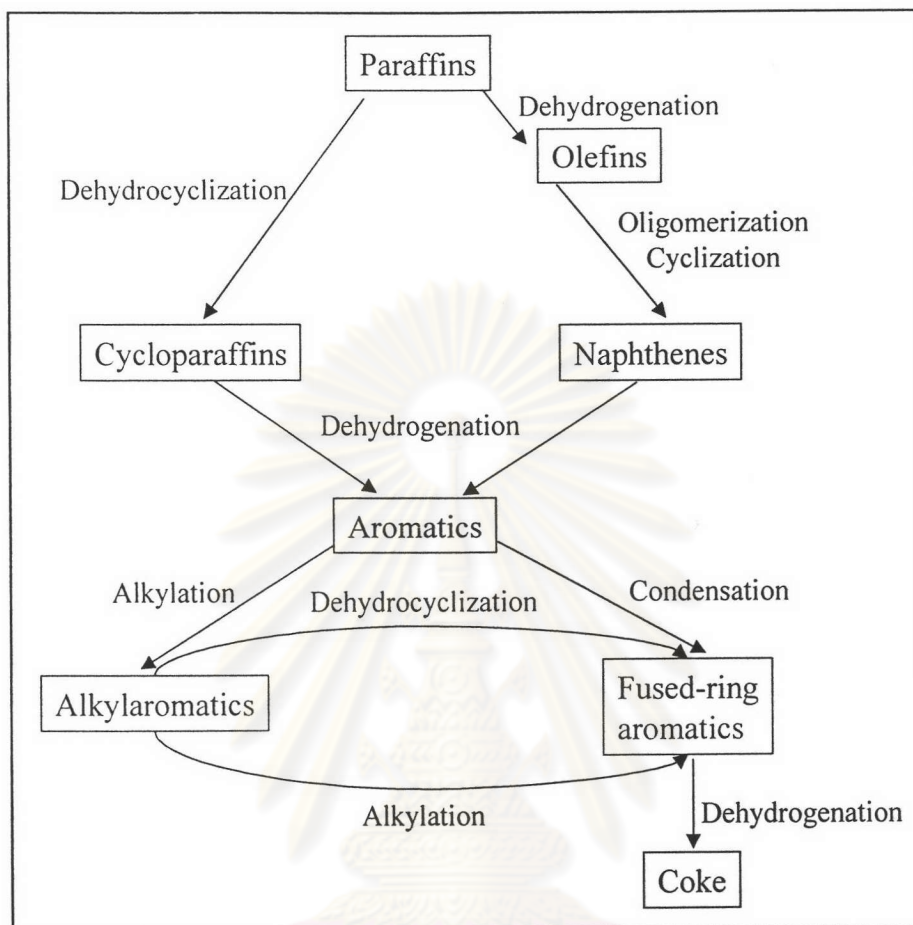
Huger *et al.* supported the “hydrocarbon pool” mechanism in MTO process by studying *in situ* MAS NMR spectroscopy on H-ZSM-5,⁹¹ SAPO-18 and SAPO-34⁹² under continuous flow conditions coupled with a simultaneous analysis of the reaction products by on-line GC. This new technique allows the investigation of intermediates occurring on the catalyst surface in the steady state of a reaction. A preferential formation of ethylene and propylene was observed. Simultaneously recorded *in situ* ^{13}C NMR spectra showed signal at 12-25 ppm and at 125-131 ppm for H-ZSM-5, and 126-135 ppm for SAPO-

18 and SAPO-34 indicating that the presence of adsorbed C₄-C₆ olefins. No hint for the presence of ethoxy, propoxy or butoxy groups and the formation of alkyl oxonium ions were found. All these supported the “hydrocarbon pool” mechanism.

2.10.2 Coke Formation in MTO process

The deactivation of catalysts in hydrocarbon processing was an enduring problem, and not only from an industrial point of view.⁹³ If deactivation of zeolite catalysts was caused by the formation of carbonaceous deposits (so called “coke”) on the catalyst surface, the original activity of the catalyst may be restored by a combustion with oxygen. However, this type of oxidative regeneration resulted in the treatment of catalysts with water at high temperatures. Especially in the case of zeolite catalysts, such a procedure may lead to irreversible changes in the structure and composition of catalysts. Moreover, in the case of large-scale fixed-bed reactors, catalyst regeneration was always a troublesome and time-consuming task if uncontrolled, hazardous coke burning was to be avoided. Therefore, many efforts have been made to reduce the deactivation rate and to prolong the time on stream by varying the reaction conditions and modifying the catalyst.

Coke⁹⁴ is the generic name given to nonvolatile and usually undesirable organic compounds which are formed in or on catalysts during operation and which block access to active sites, thereby causing catalyst deactivation. Scheme 2.14 reveals coke deposition in zeolites.³⁶ Coke, which should be considered as a mixture of hydrogen deficient residues, originates mainly from aromatics and/or olefins and aromatic-ring alkylation or hydrogen-transfer reactions are highly important contributors to coke deposition. Coke would already be formed at early stages of methanol conversion and would cover the strong acid sites. There are numerous papers concerning the effects of the pore structure of the zeolites, the aluminum content and crystal size as well as reaction temperatures on the coke formation rate and location and nature of coke species.

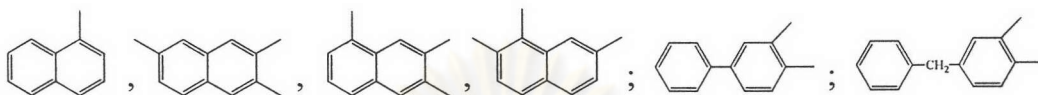


Scheme 2.14 Coke deposition in zeolites.³⁶

One of the major advantages of ZSM-5 which having MFI structure when compared with other zeolites was its high resistance to deactivation by coke formation.⁶ It was early recognized that intracrystalline coke formation on zeolites is a shape selectivity reaction, directly related to the pore structure. By comparing coke formation on ZSM-5 and mordenite in the methanol conversion it was clearly demonstrated that the low selectivity towards coke formation on ZSM-5 must arise from structural constraints on the reaction of the same intermediates of coke. In addition, Ione *et al.*⁶ studied the effect of the Si/Al ratio on the coke formation on ZSM-5 in methanol conversion. It was found that an increase in the

production of aromatic, which in turn resulted in a faster deactivation, was observed with decreasing Si/Al ratio (increasing acid strength).

Schulz *et al.*⁹⁵ studied the reaction of coke formation from methanol on ZSM-5 catalysts. As main constituents of the coke that was found dimethyl- and trimethyl naphthalenes like alkyl biphenyl and alkylate biphenyl methane.



It is concluded that the coke in the pore of H-ZSM-5 preferentially consisted of two ring aromatics.

ศูนย์วิทยทรัพยากร
จุฬาลงกรณ์มหาวิทยาลัย